HUMID TERMINAL SPLAYS AS SAND-SHEET RESERVOIRS: A FIRST LOOK AT THE MODERN, ANDEAN FORELAND, AND A NEW LOOK AT THE ANCIENT, RATON BASIN

by

Graham Edward McGregor

B.S. Geology, 2015
University of Texas at Austin
Austin, Texas

Submitted to the Graduate Faculty of the
College of Science and Engineering
Texas Christian University
in partial fulfillment of the requirements
for the degree of

Master of Science in Geology

December 2017

ACKNOWLEDGEMENTS

First and foremost, I'd like to thank Dr. John Holbrook for providing me with the opportunity to learn and grow as a geologist during my time at Texas Christian University. I would also like to thank Pioneer Natural Resources for helping to make this project possible, as well as my thesis committee, Bo Henk and Dr. Richard Denne for your guidance in this process. Next, a huge thank you goes to my parents, Bill and Katherine McGregor for all of your love and support in everything I do. I'd like to acknowledge and thank several of my friends and colleagues for their help while out in the field: Cody Myers, Nicole Wilson, Paula Santi Malnis, and Robbie Horner. Additionally, I want to thank Michael Glass and the rest of the TCU IT Helpdesk. Thank you all for being so generous with your time and efforts, I truly couldn't have done it without your help. Last but not least, I'd like to thank my Lord and Savior, Jesus Christ, whom without none of this would be possible.

Table of Contents

Acknowledgements……..ii

List of Figures……..v

List of Tables……..ix

I. Introduction…….....1

I.1 Geologic Background…….....2

I.1.1 Field Areas…….....2

I.1.2 Distributive Fluvial Systems……..10

I.1.3 Terminal Splays…….14

II. Methods…….16

III. Data and Results……21

III.1 Campichuelo Terminal Splay Complex…….21

III.1.1 Campichuelo Terminal Splay Complex: Deposition……..21

III.1.2 Campichuelo Terminal Splay Complex: Facies…….32

III.1.2.1 Terminal Splay Sand Sheet……..32

III.1.2.2 Intersplay Deposits……...34

III.1.2.3 Channel Deposits…….34

III.1.2.4 Flood Plain Mud-flat (Mollisol)……..35

III.1.3 Campichuelo Terminal Splay Complex: Architecture…...35

III.1.4 Campichuelo Terminal Splay Complex: Vegetation…….50

III.2 Raton Formation Terminal Splay Complex……..53

III.2.1 Raton Formation Terminal Splay Complex: Facies……...53

III.2.1.1 Terminal Splay Sand Sheet……..53

III.2.1.2 Intersplay Deposits……..56

III.2.1.3 Channel Deposits…….58

III.2.1.4 Flood Plain Mud-flat and Swamp……....58

III.2.2 Raton Formation Terminal Splay Complex: Architecture..59

IV. Discussion……..64

IV.1 Campichuelo and Raton Formation Terminal Splay Comparisons...64

IV.2 Terminal Splay Complex Depositional Process……65

IV.3 Implications for Petroleum Extraction……..70

V. Conclusion…….71

References……..73

Appendix……77

Vita

Abstract

List of Figures

Figure 1.1 Local map of the Raton Basin……3

Figure 1.2 Raton Basin stratigraphic column……..4

Figure 1.3 DFS development……...6

Figure 1.4 Raton Formation depositional model…….7

Figure 1.5 Cretaceous paleogeographic map……...8

Figure 1.6 Modern analog aerial map……..9

Figure 1.7 DFS model……11

Figure 1.8 DFS schematic map……..12

Figure 1.9 DFS regional model……..12

Figure 2.1 “Lower Valdez” outcrop……...17

Figure 2.2 Dutch Auger method……18

Figure 2.3 CTS aerial map…….19

Figure 2.4 Unclean river exposure…….20

Figure 2.5 River exposure cleaning……...21

Figure 2.6 River exposure cleaning……...21

Figure 3.1 CTS aerial map 1984 ……...24

Figure 3.2 CTS aerial map 1985……24

Figure 3.3 CTS aerial map 1987……25

Figure 3.4 CTS aerial map 1998 ……...25

Figure 3.5 CTS aerial map 1990 ……...25

Figure 3.6 CTS aerial map 1991 ……...26

Figure 3.7 CTS aerial map 1992 ……...26

Figure 3.8 CTS aerial map 1995 ……...26

Figure 3.9 CTS aerial map 1996 ……...27

Figure 3.10 CTS aerial map 1997 ……27

Figure 3.11 CTS aerial map 1999 ……27

Figure 3.12 CTS aerial map 2000 ……28

Figure 3.13 CTS aerial map 2002 ……28

Figure 3.14 CTS aerial map 2003 ……28

Figure 3.15 CTS aerial map 2004 ……29

Figure 3.16 CTS aerial map 2005 ……29

Figure 3.17 CTS aerial map 2006 ……29

Figure 3.18 CTS aerial map 2007 ……30

Figure 3.19 CTS aerial map 2008 ……30

Figure 3.20 CTS aerial map 2009 ……30

Figure 3.21 CTS aerial map 2010 ……31

Figure 3.22 CTS aerial map 2014 ……31

Figure 3.23 CTS aerial map 2016 ……31

Figure 3.24 Buried, *in-situ* tree……..33

Figure 3.25 Buried, *in-situ* tree……..33

Figure 3.26 Sample of mollisol horizon……35

Figure 3.27 CTS river exposure locations……36

Figure 3.28 Face 1……38

Figure 3.29 Face 2……39

Figure 3.30 Face 3……40

Figure 3.31 Face 4……..41

Figure 3.32 Face 5……..42

Figure 3.33 Face 6……..43

Figure 3.34 Face 7……..44

Figure 3.35 Face 8……..45

Figure 3.36 Cross-section A-A'…….47

Figure 3.37 Cross-section B-B'…….48

Figure 3.38 Cross-section C-C'…….49

Figure 3.39 CTS vegetation and uprooted tree……..50

Figure 3.40 CTS uprooted tree……..51

Figure 3.41 CTS charred tree……51

Figure 3.42 CTS charred tree……52

Figure 3.43 CTS charred tree……52

Figure 3.44 Vegetation interaction in downstream view of CTS……..53

Figure 3.45 CTS tree acting as obstacle……53

Figure 3.46 Raton palm tree……..54

Figure 3.47 Raton palm tree and root ball…….55

Figure 3.48 Raton palm frond……...55

Figure 3.49 Raton rhizoliths……..56

Figure 3.50 Raton organic leaf……..57

Figure 3.51 Raton coalified taproot……...57

Figure 3.52 Vertically exaggerated Lower Valdez section……...60

Figure 3.53 Lower Valdez sedimentary structures……....61

Figure 3.54 Raton channel deposit sedimentary structures……...62

Figure 3.55 Raton terminal splay sedimentary structures…….63

Figure 3.56 Raton terminal splay sedimentary structures…….63

Figure 3.57 Raton terminal splay sedimentary structures…….64

Figure 4.1 Raton and CTS complex comparison……..70

List of Tables

Table 3.1 Sedimentary structures……37

I. Introduction

Thin sand sheets deposited in the distal zone of a distributive fluvial system (DFS; after Nichols and Fisher, 2007), have potential to serve as laterally connective hydrocarbon reservoirs promoted by high accommodation rates within the basin. Later flooding events lead to mud deposition, forming seals over the top of the laterally connected sand bodies (e.g., Lang et al, 2004). The thin sandstone sheets studied in the ancient and modern analogs in this study bear the characteristics of humid terminal splays. I predict that the sedimentary architecture and internal sedimentary structures of the ancient sand sheets in the Raton Formation will share sufficiently common traits to modern terminal splays. The hypotheses will be tested by analyzing and comparing architecture and facies associations in modern terminal splays of northern Argentina and sand sheets in the Raton Formation.

Characterization of thin beds in the Raton Formation will support ongoing gas production in the Raton Basin. Abundant coal seams throughout the Vermejo and Raton Formations support coal bed methane production in the Trinidad, Colorado area. Terminal splay sand bodies offer potential as currently unutilized secondary reservoirs. Production could be enhanced if terminal splays prove viable as reservoirs. Understanding production potential for these sands depends on a meaningful predictive understanding of the reservoir geometry and connectivity. This is not feasible in the absence of a geologic model that captures the origin and characteristics of these strata. The shale and coal seals that form over the top and beneath the splays can serve as a source and seal for these potential reservoirs. Better knowledge of the origin and

characteristics of terminal splays will guide future exploration efforts in the Raton and other basins.

I.1 Geologic Background

I.1.1 Field Areas

The Raton Basin: The Raton Basin is an asymmetric syncline covering approximately 2,500 square miles extending from its northern extent of Huerfano Park, Colorado to the southern extent near Cimarron, New Mexico. The Raton Basin is bound by the Wet Mountains to the north and the Cimarron Mountains to the south. The San Luis Highlands (i.e. the Sangre de Cristo Mountain Range) bound the basin to the West, and the Sierra Grande, Las Animas, and Apishapa arches to the East (Figure 1.1) (Johnson et al., 1956; Baltz, 1965; Flores, 1987; Flores and Pillmore, 1987). The basin fill ranges in age from Late Cretaceous to early Tertiary and represents the deposition of marine, coastal, and alluvial sediments through syntectonic infilling during the Laramide Orogeny following the retreat of the Cretaceous Western Interior Seaway (Pillmore and Mayberry, 1976; Billingsley, 1977; Flores and Tur, 1982; Flores, 1987; Pillmore and Flores, 1990).

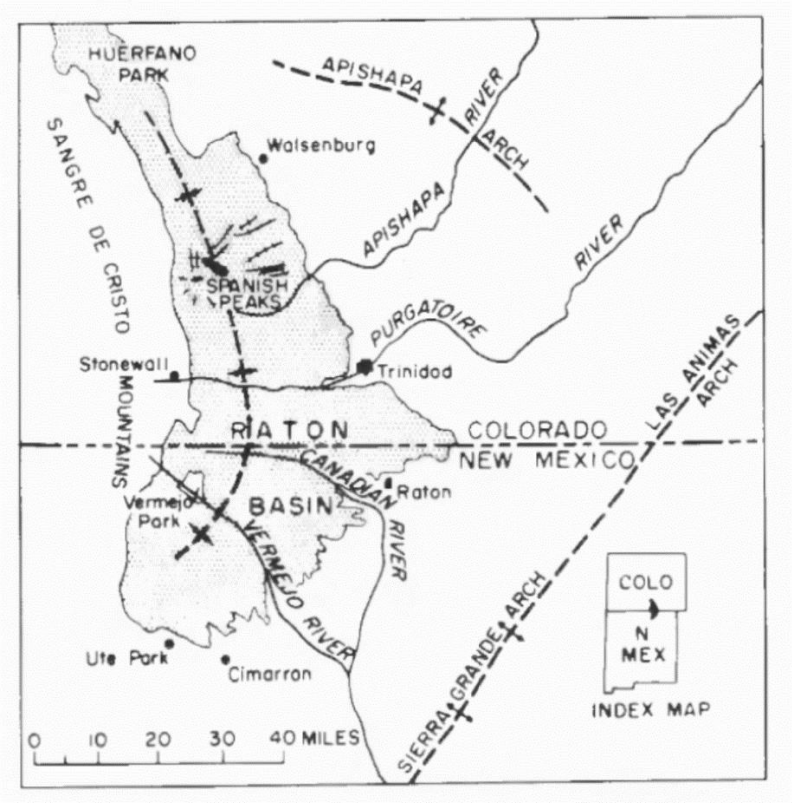

<u>Figure 1.1</u> Local map of the Raton Basin in Southern Colorado and Northern New Mexico (Flores, 1987).

The Raton Basin fill comprises five stratigraphic units (Figure 1.2), two are marine and three are non-marine. The oldest unit in the basin is the Pierre Shale, dated to Campanian – Maastrichtian based on ammonite fossils (Scott and Pillmore, 1989; Pillmore and Flores, 1990). The Pierre Shale is a 1,800 – 1,900-foot-thick dark, silty, noncalcareous shale, deposited in prodeltaic and offshore marine environments of the Western Interior Cretaceous Sea prior to marine retreat. The Pierre Shale intertongues with the Trinidad Sandstone and transitions through about ten feet of interbedded shale and siltstone with sandstone beds containing marine *Ophiomorpha* traces appearing at the end of the transition and continuing upward throughout Trinidad strata (Pillmore and Flores, 1990).

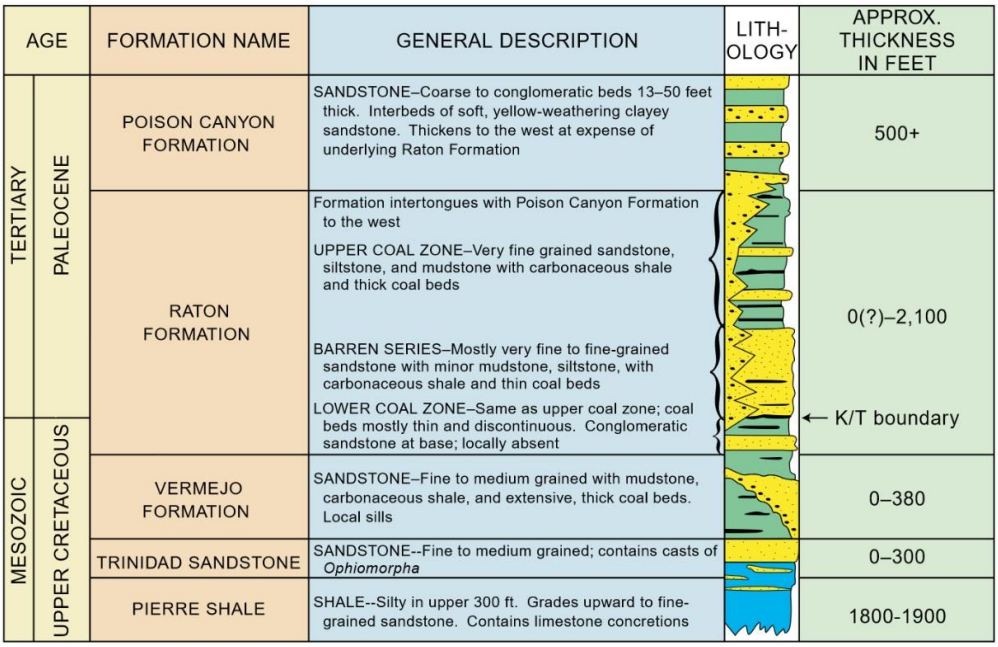

Figure 1.2 Stratigraphic column making up the Raton Basin (Pillmore, 1969; Flores, 1985; Flores, 1987; Pillmore and Flores, 1987; Johnson and Finn, 2001).

The Trinidad Sandstone is a cliff-forming unit characterized by tabular sand bodies up to 300 feet thick. As the Cretaceous shoreline prograded, fine- to very fine-grained sandstone deposited in upper and lower delta-front environments (Billingsley, 1977). The Trinidad Sandstone is truncated by the Raton Formation locally to the west, but is generally overlain by the Vermejo Formation (Johnson and Wood, 1956; Pillmore and Flores, 1990). Trace fossils including *Ophiomorpha* and *Diplocraterion* are present in the formation (Pillmore and Maberry, 1976). The marine to non-marine depositional environment transition during the Late Cretaceous is represented by the Vermejo Formation. Nearly 400 feet of interbedded sandstone, siltstone, shale, carbonaceous shale, and coal layers were deposited conformably over the top of the Trinidad Sandstone in both fluvio-deltaic and back-barrier plains (Billingsley, 1978; Pillmore and Flores,

1990). The channel margin was filled with fresh water distributary channels, evidenced by a lack of marine fauna (Billingsley, 1977).

The Raton Formation was deposited on an alluvial plain from latest Cretaceous into the early Tertiary, and is divided into three subdivisions reaching up to 2,100 feet of total thickness. The first of the three, the lower coal zone, is composed of mudstone, siltstone, carbonaceous shale, and coal beds, interbedded with the channel bodies (Pillmore and Flores, 1990) and the thin sand sheets targeted in this study. The K-T boundary is very well preserved in this zone.

The barren series is deposited on top of the lower coal zone and overlain by the upper coal zone. The barren series is a sequence of thick channel sandstones stacked vertically with minimal coal. Above the barren series is the upper coal zone, which is similar to the lower coal zone in that it is composed of siltstone and mudstone interbedded with channel sands, thin sheet sandstone, carbonaceous shale, and thick coal seams (Pillmore and Flores, 1990). The depositional environment of the lower coal zone is previously interpreted as a meandering fluvial system (Figures 1.3A and 1.3B), while that of the barren series is interpreted as a mixed braided and meandering river system (Figure 1.3D) (Pillmore and Flores, 1990). The last unit in the Raton Basin is the Poison Canyon Conglomerate, a coarse to conglomeratic arkosic sandstone. The Poison Canyon deposited in braided to meandering fan systems in an alluvial plain with a high gradient (Strum, 1984; Pillmore and Flores, 1990).

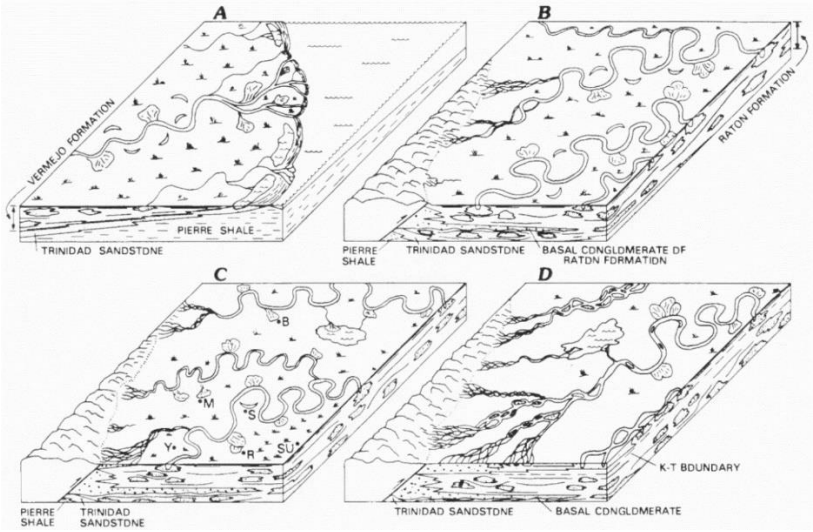

Figure 1.3 Development of the distributary fluvial system and its surrounding environments during the deposition of (A) the Pierre Shale, Trinidad Sandstone, and Vermejo Formation; (B) the lower coal zone of the Raton Formation; (C) the end of the lower coal zone of the Raton Formation; and (D) the braided and meander belts of the Raton Formation's barren series (Pillmore and Flores, 1987).

The Raton Formation deposited in response to Laramide uplift and foreland loading as eroded sediments from the Sangre de Cristo Mountains were transported in a fluvial system into the Raton Basin (Flores, 1987). Flores and Pillmore (1987) presumed that braided streams occupied the upstream section of this system, whereas meandering and anastomosing belts formed downstream due to flow and discharge decreasing as fine sediments are deposited and smeared widely across the alluvial floodplain (Flores and Pillmore, 1987) (Figure 1.4). Their proposed transition from higher to lower elevation and braided to meandering and anastomosing rivers is also characteristic of a distributive fluvial system. As sediments are carried further downstream, the river loses energy and channel belts begin to meander and eventually avulse and/or birfurcate, distributing sediments over the vegetated floodplain (Hartley et al, 2010).

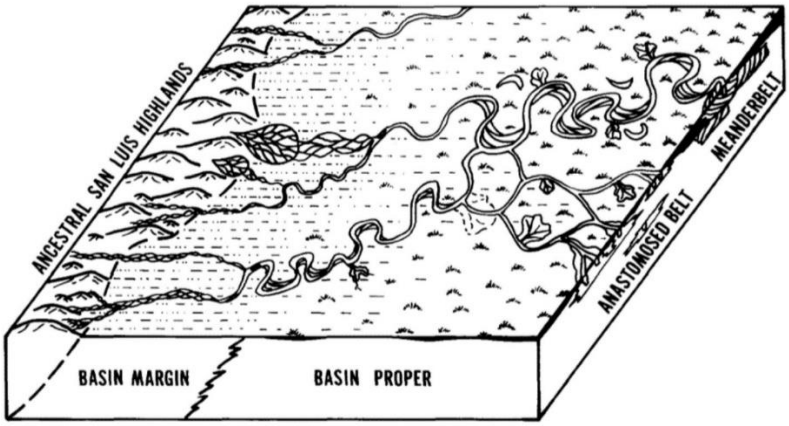

<u>Figure 1.4</u> Depositional model depicting the distributary fluvial system that deposits the coal rich zones and terminal splay sand sheets of the Raton Formation (Flores and Pillmore, 1987).

When deposition of the Raton Formation began in the Late Cretaceous, the Raton Basin sat at approximately 30° N and was in a tropical environment with high temperatures (Figure 1.5). Tropical fossilized trees are abundant throughout the Raton Formation. Arid terminal splay deposits are well studied in modern environments, but modern humid terminal splays remain uninvestigated. The Rio Seco distributive fluvial system in the northern Argentina Andean Foreland, is the site selected as a modern analog for humid/tropical terminal splays.

Figure 1.5 Paleogeographic reconstruction of North America during the Cretaceous ~65 Ma. The Raton Basin is outlined by the red circle. (Horner, 2016; Modified from Blakey, 2013)

The Rio Seco, Northern Argentina: The modern analog is located near the small community of Campichuelo, in the northern most part of Argentina along the Rio Seco, a tributary of the larger Rio Bermejo distributive fluvial system (Figure 1.6). This study focuses on a smaller discrete terminal splay adjacent to the larger terminal splay complex.

The Raton terminal splay sand sheets exhibit nearly all of the same sedimentary structures as the CTS, vertically and laterally. Despite not having insight to downstream trends or variation, I propose that the same processes have occurred in the Raton Formation.

<u>Figure 1.6</u> Aerial map of the study area in northern Argentina. Located in this area is the Rio Bermejo DFS, the Rio Seco tributary, and two terminal splay complexes (CTS & DTS) at the Rio Seco's terminus.

Similar to the Raton fluvial system in Colorado, this system transports eroded sediment from the uplifted Andean mountain range from NW to SE into the Chaco foreland basin. The formation of the Andes is attributed to crustal thickening by thrusting, coupled with extreme magmatic events (McGlue et al, 2016). As the Nazca and South American plates merged and subducted to the east, South America experienced flexure-inducing topographic and dynamic loads (Jordan, 1995; DeCelles and Giles, 1996; Chase et al, 2009; DeCelles, 2012; McGlue et al, 2016) which created a large, "laterally mobile" foreland basin adjacent to the Subandean thrust belt (Horton and DeCelles, 1997; McGlue et al, 2016). The terminal splay complex in the Chaco foreland basin is in a topographic low, with vegetation dominated by Yungas montane (subtropical

forest vegetation), and a mean annual precipitation of ~1,100 mm/year (Olson et al, 2001; McGlue et al, 2016).

The many tributaries of the Rio Bermejo drain the south-central Andean hinterland as it flows in a southeastern direction (McGlue et al, 2016). The discharge rates of the Rio Bermejo vary greatly throughout the year, ranging from 20 – 14,000 m^3/s, with around 75% of flow typically occurring during one season (Varis et al, 2008; Smith et al, 2016; McGlue et al, 2016). Annually, the Rio Bermejo deposits approximately 100 x 10^6 tons of sediment with ~98% of its sediment deposited from suspended load (Smith et al, 2016; McGlue et al, 2016).

I.1.2 Distributive Fluvial Systems

Distributive fluvial systems characterize continental subsiding basins (Weissmann et al, 2013) and are presumed here to have characterized the Raton Formation. A distributive fluvial system is a river system in which water and sediment discharge, grainsize, and river gradient decrease downstream into a distal low-gradient zone. The DFS model in Figure 1.7 (Weissmann et al, 2013) illustrates four downstream trends: increasing accommodation to sediment ratio, decreasing sand to mud ratio, sand body amalgamation, and distributive drainage. They are characterized by distributive channel bifurcation and avulsion and commonly form terminal splays at the end of channels on either a dry alluvial plain or into a lake basin. These systems commonly form in basins with a climate that is sufficiently warm and dry to promote net down-dip water loss (Nichols and Fisher, 2007), but can also form in tropical, subtropical, continental, and polar environments (Hartley et al, 2010). Distributive fluvial systems can be found in four tectonic settings: extensional, compressional, strike-slip, and cratonic (Hartley et al,

2010). Both the Paleocene Raton and modern Argentinian examples are representative of a subtropical to tropical environment.

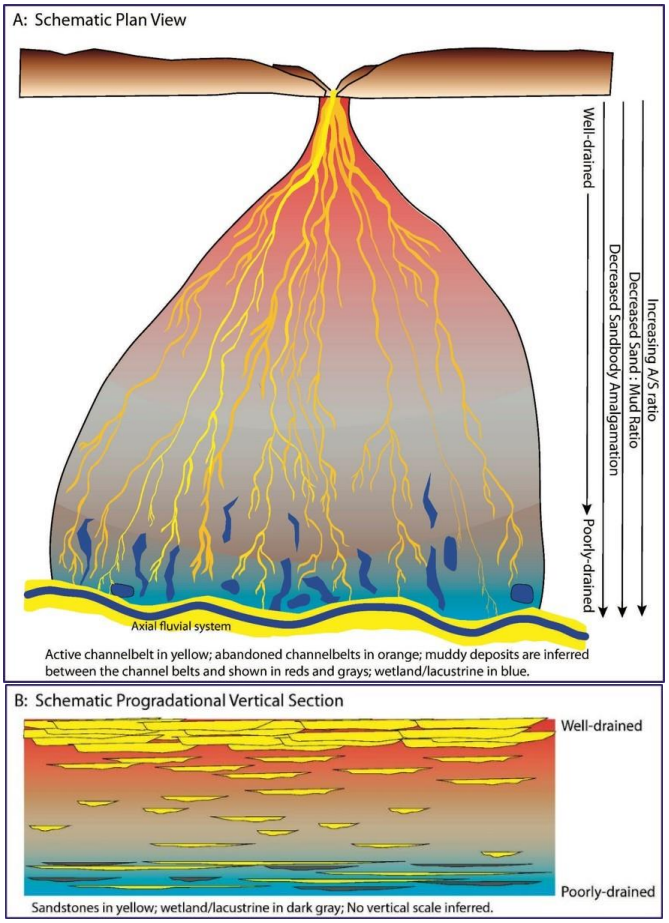

<u>Figure 1.7</u> Distributive Fluvial System model developed by Weissmann et al, 2013. A) Illustrates downstream trends of the DFS: increasing accommodation to sediment ratio, decreased sand to mud ratio, decreased sand body amalgamation and decreased drainage; DFS and terminal splay complex terminated at the axial fluvial system of the larger DFS. B) Cross-sectional view illustrating the downstream trends of the system.

The length of the fluvial system is governed by basin size, as well as the relationship between the amount of water supplied and the amount of water lost throughout the system due to evaporation and infiltration (Nichols and Fisher, 2007). Distributive fluvial systems form a radial pattern, spreading out across the alluvial plain (Nichols and Fisher, 2007). The three zones that make up a DFS include: a proximal zone, a medial zone, and a distal zone (Figures 1.8 and 1.9; Nichols and Fisher, 2007).

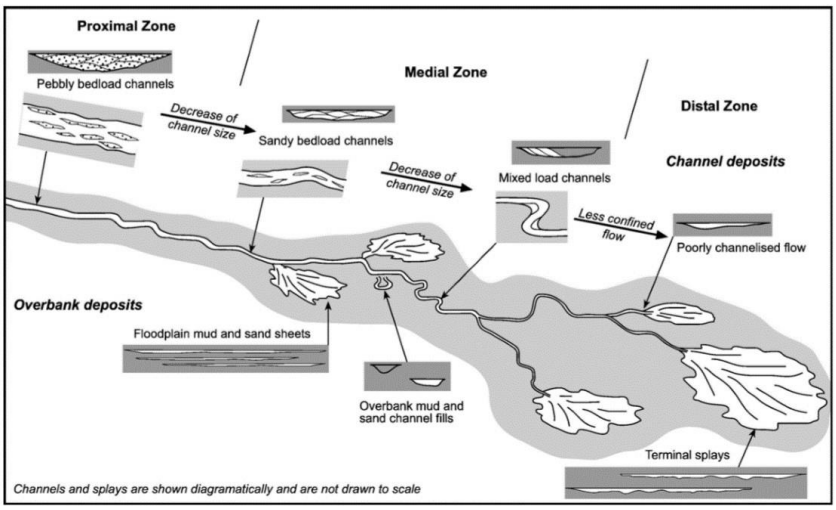

Figure 1.8 Schematic map of a distributary fluvial system illustrating the characteristics and features typically formed (Nichols and Fisher, 2007).

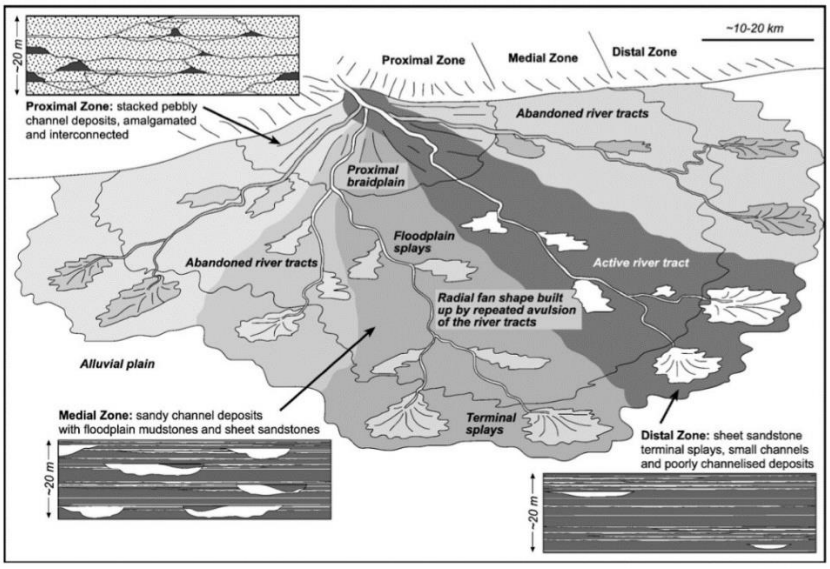

Figure 1.9 Regional depositional model of a distributary fluvial system (Nichols and Fisher, 2007)

The proximal zone represents the point at which the channels are largest and most deeply incised, and possess the largest grain sizes (Nichols and Fisher, 2007). These zones are typified by amalgamated coarse, pebbly and sandy channel deposits, and do not preserve overbank facies well. Proximal strata are coarse sand or conglomeritic facies with clast imbrication, cross-beds and bar structures leading commonly to the interpretation that these strata are deposited by braided streams near the basin margin

(Graham, 1983; Nichols, 1987; MacCarthy, 1990; Sadler and Kelly, 1993; Nichols and Fisher, 2007). Overbank preservation is uncommon here and the channel belts are amalgamated. Nichols and Fisher (2007) concluded that these proximal channels were laterally migrating, resulting in floodplain deposits being reworked by repeated avulsion.

Channel-fill bodies in the medial zone are more stable laterally (MacCarthy, 1990; Hirst, 1991) and overbank facies are better preserved (Figures 1.8 and 1.9). Grain size within the channel-fills is generally finer compared to the proximal zone (Nichols and Fisher, 2007). The overbank facies deposited in medial zones form soils which indicate drainage to extreme dryness (Graham, 1983; Nichols and Fisher, 2007). Sandstone sheets accompany channels and are typically a few centimeters thick and extend laterally over tens of meters (Nichols and Fisher, 2007). These laterally extensive beds are characterized by a sharp base, locally containing current ripple cross-laminations, and are separated throughout by overbank mudstone packages (Nichols and Fisher, 2007).

The most distinctive elements of DFS systems form in the distal zone. The distal zone is abundant with floodplain facies and sparse channel-fill deposits that are typically shallow and undefined, (Graham, 1983; Sadler and Kelly, 1993; Nichols and Fisher, 2007) and characterized by unchannelized flow (Nichols and Fisher, 2007). Channel scours found in these zones are typically partly or fully filled with mudrock, which suggests localized channelization (Graham, 1983; Nichols and Fisher, 2007). Channels are less laterally-mobile which gives vegetation on the floodplain a chance to make channel banks more stable (Nichols and Fisher, 2007). If the river cannot maintain flow across the basin, they will terminate within the basin (Hartley et al, 2010) and deposit

terminal splay complexes onto the alluvial floodplain. Laterally extensive sheets, interpreted as terminal splays form in distal zones and are bounded by thick, muddy and silty units with paleosols (Sadler and Kelly, 1993; Fisher et al., 2006; Nichols and Fisher, 2007). The distal zone has a decrease in slope, size of channels, and sediment capacity owing to bifurcation, infiltration, and evapotranspiration (Hartley et al, 2010). The characteristics of the DFS' distal zone as described here are very similar to the environment seen in the Raton Formation, including the abundant amount of trace fossils and rooting suggesting a vegetated floodplain.

I.1.3 Terminal Splays

Terminal splay sand bodies typical in distal areas of a DFS are poorly understood in humid environments but better studied in arid systems. Terminal splays are defined in arid environments (Fisher et al, 2008) as lobe-shaped bodies of sediment found at the end of a river, deposited from unconfined, sub-aerial sheet floods spreading over a dry floodplain, playa, or lake bed. The distal zone at the end of the DFS is characterized by thin sheets of sand presumed to be terminal splays (Figure 1.9) exhibiting lateral connectivity with beds of mud and siltstone hosting paleosols (Sadler and Kelly, 1993; Fisher et al, 2006; Nichols and Fisher, 2007). Lang et al (2004) found terminal splays in dryland environments of Australia are formed where there is no standing body of water as flows quickly come to a halt with lost slope.

Terminal splay complexes have considerable reworking but preservation of discrete splays is still common. The beds that are deposited either exhibit high or low net-to-gross fluvial terminal splay sand sheets, interpreted to be deposited during falling

stages of flooding (Lang et al, 2004). Falling stage promotes preservation for the splay bodies as there is less of a chance for reworking. At the end of flooding, mud deposits accumulate and isolate the reservoir sands (Lang et al, 2004). Where accommodation is slow, connectivity within the sands should be greater and discrete splays more poorly preserved with less accommodation space. That being said, the floodplain deposits may serve as good seals for the connected sand bodies where formed (Lang et al, 2004).

Sedimentary structures of terminal splay sandstone sheets include parallel laminations, convex-upward parallel laminations, climbing ripples, and small scale dunes (Lang et al, 2004). Terminal splays studied by Nichols and Fisher exhibit horizontal stratification, current ripple laminations, and localized dune structures. Sadler and Kelly's study (1992) concluded that these deposits are mostly parallel and/or ripple cross-laminated, with a local massive sandstone. These are all examples of terminal splay complexes in arid environments.

Fielding (2006) found similar sedimentary structures in subtropical river deposits that are broken down into five bedding types: sigmoidal to low angle bedding exhibiting low angle cross-sets; parallel planar bedding; low angle beds exhibiting some convex-upward laminations; convex-upward beds with low angle cross-lamination and symmetrical drapes; and up-dip terminating backsets against an upstream erosion surface. Fielding concluded the sigmoidal to low angle bedding with low angle cross-sets records the transition from dune to the upper plane bed of upper flow regime, which is represented by parallel planar laminations. Parallel planar upper plane flow transitions into the antidune stability field indicated by low angle beds exhibiting some convex-upward laminations. The antidunal stability field is characterized by convex-upward beds

with low angle cross-bedding and symmetrical drapes. Chute and pool conditions form as the channel meanders, creating up-dip terminating backsets against an upstream erosional surface (Fielding, 2006).

II. Methods

Field work in the Raton Formation focused on the "Lower Valdez" outcrop. The Lower Valdez outcrop (Figure 2.1) is the best example of the Raton Formation sand sheets, previously mapped by Horner (2016) for general facies distribution. The outcrop runs along Highway 12, and is approximately 310 meters long with a large symmetrical channel complex in the middle. The section also has a succession of thin, laterally extensive sand sheets with even thinner layers of mud and silt between sand sheets. Seven vertical sections were measured through this section and spaced along the outcrop length. From right to left, 50 meter intervals were measured between each vertical section; excluding the last section taken 30 meters away from the previous section. Connectivity and internal characteristics are the focus of observation for the sand sheets, including: sedimentary structures, lithology, grain size, architecture, and vegetation fossils. Measured sections (Figure 2.1) range from 1.54 to 5.53 meters thick.

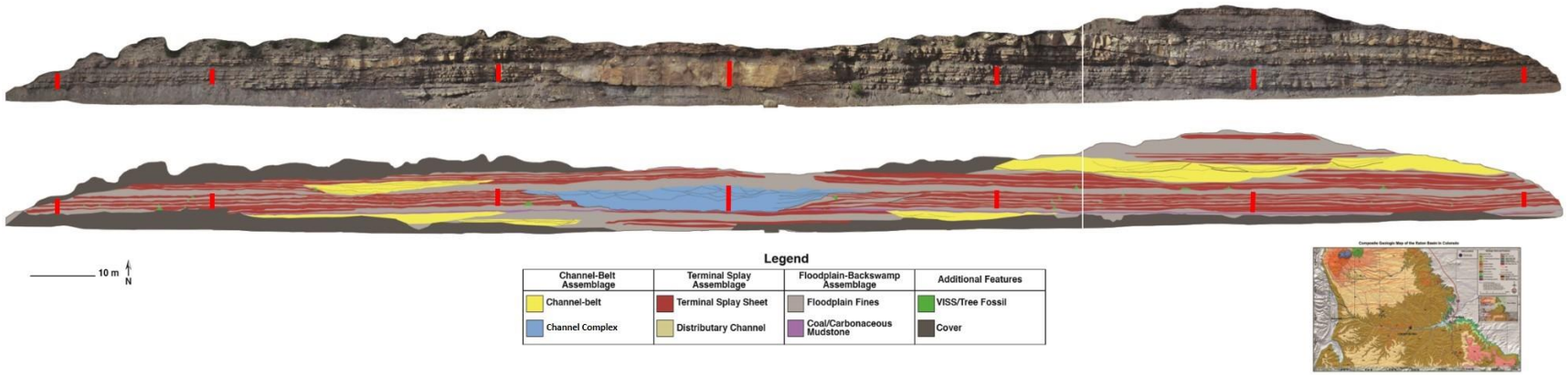

Figure 2.1 "Lower Valdez" outcrop. Depicted in this outcrop are: channel-belts, channel complex, terminal splay sheets, distributive channel, floodplains, mudstones, vegetation induced sedimentary structures, and cover. The red line in the top image indicates the locations of the measured vertical sections. This section is ~310 meters long. (Modified from Horner, 2016).

Google Earth was used to locate an accessible and similarly scaled example of a terminal splay complex deposited in a humid environment analogues to the Raton Basin. The splay also needed to be an accessible and practical work target. These criteria led to northern Argentina near the small town of Campichuelo. This splay complex is hereafter referred to as the CTS (Campichuelo Terminal Splay).

Three cross-sections are drilled through the CTS using a Dutch Auger (Figure 2.2) to collect sediment and study grain size and composition to characterize the distribution of the CTS, and to define the stratigraphy of underlying splays. Cross-sections are located at the mouth of the splay complex (A-A'), the distal end of the complex (B-B'), and the complex's longitudinal profile (C-C') (Figure 2.3).

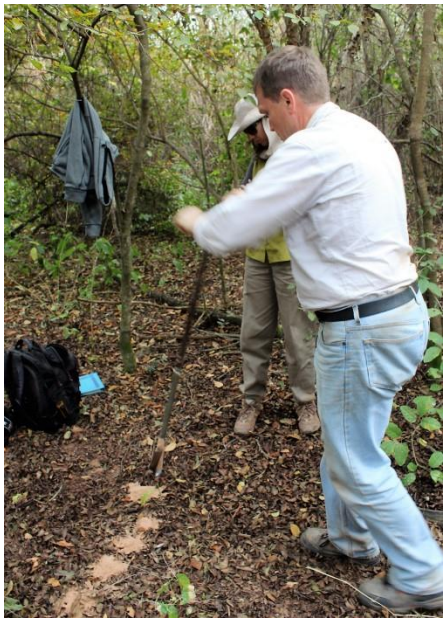

Figure 2.2 The Dutch Auger being used to pull out sediment samples in 10 centimeter intervals.

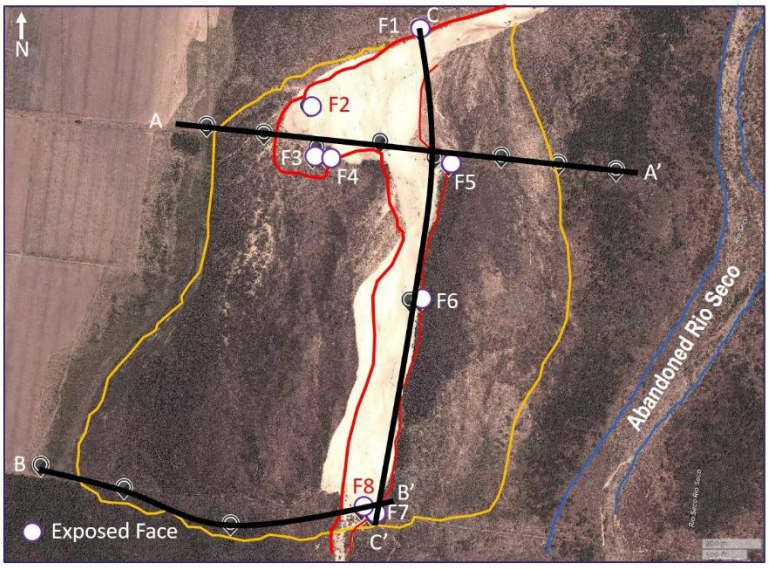

<u>Figure 2.3</u> Aerial map of the terminal splay complex in Argentina. A-A' representing the proximal cross-section, B-B' representing the distal cross-section, and C-C' representing the longitudinal cross-section. The locations where clean faces were available to examine are indicated by the white circles, whereas the black circles are locations that only logs were drilled. The orange line illustrates the extent of the CTS as it was deposited in the 2007 flooding event, and anything inside the red line was a part of the dry, sandy river bed present in August 2016. Anything outside of the red was heavily vegetated, and the blue outlines the abandoned Rio Seco Tributary.

The first cross section, A-A', covers the mouth of the splay and is perpendicular to the flow of the channel. Using the auger, logs were drilled ~3-5 meters deep over an approximate 1,400-meter distance. Eight holes were drilled and were all done ~200 meters apart. The sediments were described in 10 centimeter intervals, providing the stratigraphy of the splay complex.

Cross-section B-B' in the distal zone of the splay is based on 5 drill-hole logs using the auger over ~1,000 meters. Despite the splay extending further to the east, B-B' became too vegetated to navigate. Using the same methods as before, drilling went ~5 meters deep in 10 cm increments. From west to east, the increments between drill holes were 250 m, 350 m, 350 m, and 50 m, respectively. The longitudinal profile (C-C') was

constructed from four drill-holes used in lateral cross-sections by lining them up down the middle of the CTS, extending nearly 1,900 meters.

Sedimentary structures and internal characteristics of the terminal splay sand sheets were studied in 8 different faces originally exposed by the channel. The exposed surfaces (Figure 2.4) were dressed to highlight sedimentary structures. Initially, a shovel was used (Figure 2.5) to smooth the irregular surface, followed by the use of a machete to transform the face into a flat, uniform surface. A paint brush was then used (Figure 2.6) to delicately clean the face in order to expose the internal features of the terminal splay deposits: sedimentary structures, lithology, grain size distribution, geometry, and vegetation interaction. This method was followed on all 8 faces.

Figure 2.4 Example of an unclean face before beginning to clean it off (Face 5). In-situ tree buried through several flooding events.

Figure 2.5 Method of using a shovel to initially expose the face by cleaning off the original irregular surface (Face 3).

Figure 2.6 Paint brush being used to delicately expose all of the face's internal structures (Face 5).

III. Data and Results

III.1 Campichuelo Terminal Splay Complex

III.1.1 Campichuelo Terminal Splay Complex: Deposition

This study focuses on the most recent discrete terminal splay, deposited in 2007 according to Google Earth historical imagery. Through the use of Google Earth's historical imagery slider, a timeline of aerial photographs (Figures 3.1-3.23) of the

terminal splay complex was compiled every year on December 30th from 1984 through 2016. The faces and drill-holes expose multiple splay layers which include the uppermost 2007 CTS deposit seen in aerial view. The 2007 CTS refers to the most recent terminal splay sand sheet whereas the CTS refers to the stack of terminal splays as a complex.

By December of 1984, the Rio Seco terminated within the CTS complex, depositing a sheet of sand onto the vegetated floodplain in a radial pattern (Figure 3.1). The prograding Rio Seco incised through the CTS deposits and eventually deposited a larger distal terminal splay (DTS) complex ~3 km downstream by the end of 1985 (Figure 3.2). Vegetation begins to cover the 1984 CTS deposit through inactivity on the floodplain after flow was channelized. The channel remained active through 1987 (Figure 3.3), continuing DTS deposition at a decreasing rate. The 1984 CTS deposit was completely overgrown with vegetation by the end of 1987.

Two more sand sheets were deposited on the DTS complex in 1987-1988 (Figure 3.3 & 3.4), and became heavily vegetated due to inactivity until 1990 (Figure 3.5). Upon channel reactivation in 1990, DTS deposition continued through 1991 (Figure 3.6) at which point the extent of the DTS is seen, exhibiting a radial planform. In 1992 (Figure 3.7) the Rio Seco began to avulse and develop a lobe that lead to the deposition of the 2007 CTS sand sheet. Simultaneously, a crevasse splay deposit formed as the last DTS deposit became overgrown with vegetation. As Rio Seco avulsion continued, the mouth of the 2007 CTS deposit developed. The tributaries within a terminal splay complex are active temporarily, they are eventually abandoned and become overgrown with vegetation. The Rio Seco remained inactive through 1996 (Figure 3.9), aside from a

minor flooding event that occurred in 1995 (Figure 3.8). This event deposited a small terminal splay sand sheet in the DTS complex.

A large, elongate DTS sand sheet deposited in 1997 (Figure 3.10); confined to its channel in a linear pattern, opposed to a radial terminal splay deposit. The Rio Seco remained inactive through 1999 (Figure 3.11), and smaller vegetation covered the 1997 DTS deposit. The Rio Seco avulsed downstream in 2000 (Figure 3.12) when another flooding event deposited a terminal splay sand sheet, bounding the 1997 deposit to the east. Rio Seco inactivity through 2002 (Figure 3.13) allowed vegetation to grow atop the abandoned and inactive tributaries. Flooding that began in 2003 (Figure 3.14) extended the 2000 DTS to the south, and continued to prograde from 2004-2006 (Figures 3.15-3.17). By 2006, the most recently abandoned tributary had become completely vegetated. The prograding channel terminated in 2006 (Figure 3.17), depositing another DTS sand sheet in an elongate, radial pattern. Following deposition of the 2006 DTS, the Rio Seco avulsed upstream and began to establish the 2007 Campichuelo Termial Splay deposit.

Although the Rio Seco's avulsion began in 2006, it wasn't until 2007 (Figure 3.18) that the radial 2007 CTS sand sheet deposited. Shortly after the 2007 CTS deposition, the recently avulsed Rio Seco resumed progradation to the DTS complex. As a result, channel incision dissected the 2007 CTS sheet and exposed several CTS sand sheet deposits and left the CTS abandoned as a terrace. Upon progradation, the Rio Seco subsequently deposited another sand sheet in the DTS complex which defines its' western border. The 2007 DTS deposit migrates east and forms the mouth of the 2009 DTS deposit, while vegetation begins to grow over the 2007 CTS and DTS sands all by 2008's end (Figure 3.19).

The 2009 DTS (Figure 3.20) deposit's geometry and orientation are similar to the 2007 CTS. The sand sheet continued deposition through the end of 2010 (Figure 3.21) while vegetation ensued over inactive areas of the splay complexes. Vegetation continued to grow as the Rio Seco remained inactive through 2014 (Figure 3.22) when a small distal crevasse splay deposited. Both terminal splay complexes had nearly become completely vegetated due to the Rio Seco's inactivity by December 2016 (Figure 3.23).

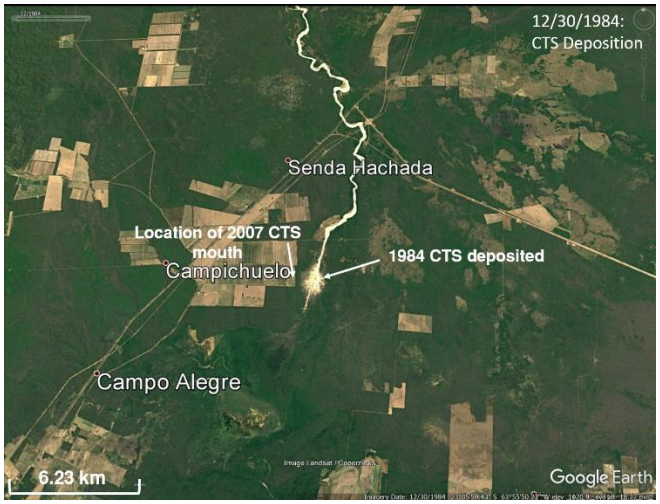

Figure 3.1 Aerial photograph of the terminal splay complex, 12/30/1984 (Google Earth).

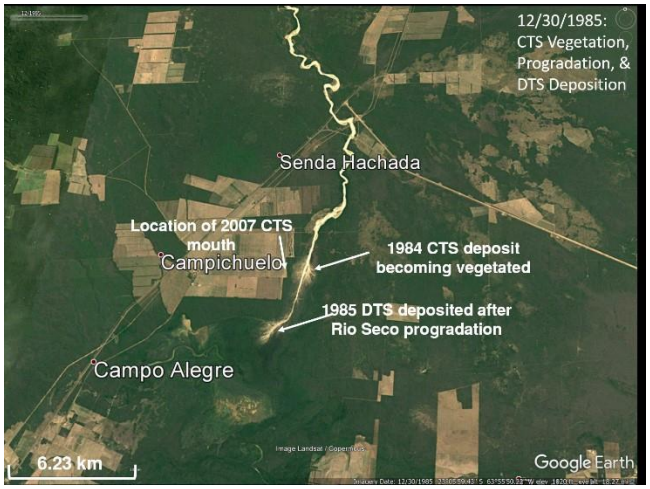

Figure 3.2 Aerial photograph of the terminal splay complex, 12/30/1985 (Google Earth).

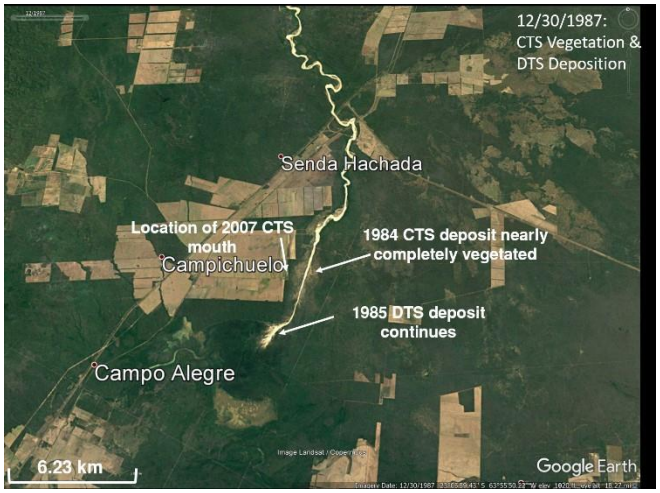

Figure 3.3 Aerial photograph of the terminal splay complex, 12/30/1987 (Google Earth).

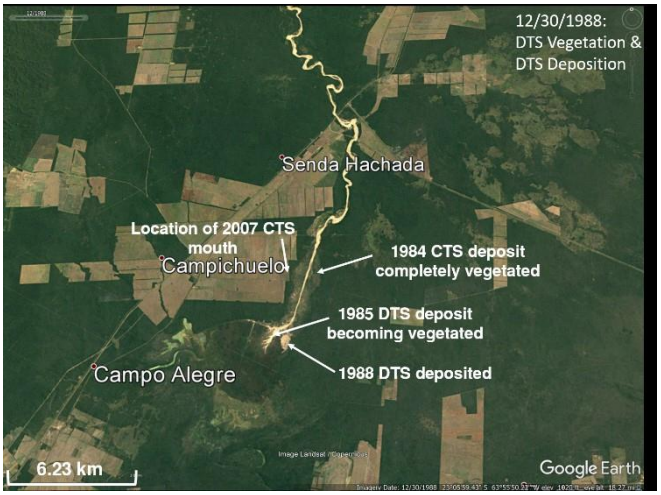

Figure 3.4 Aerial photograph of the terminal splay complex, 12/30/1988 (Google Earth).

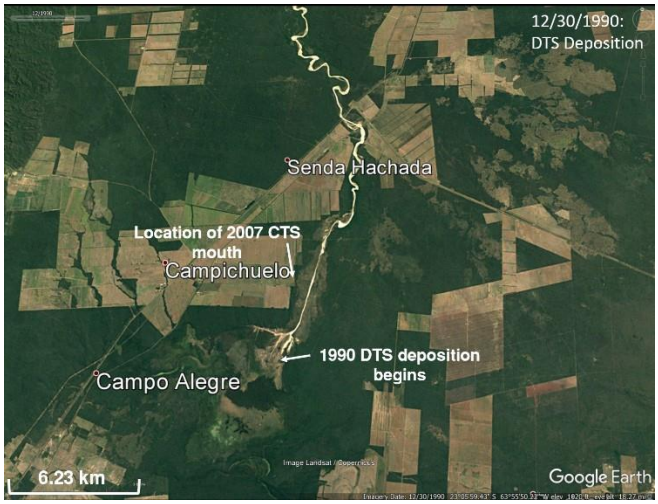

Figure 3.5 Aerial photograph of the terminal splay complex, 12/30/1990 (Google Earth).

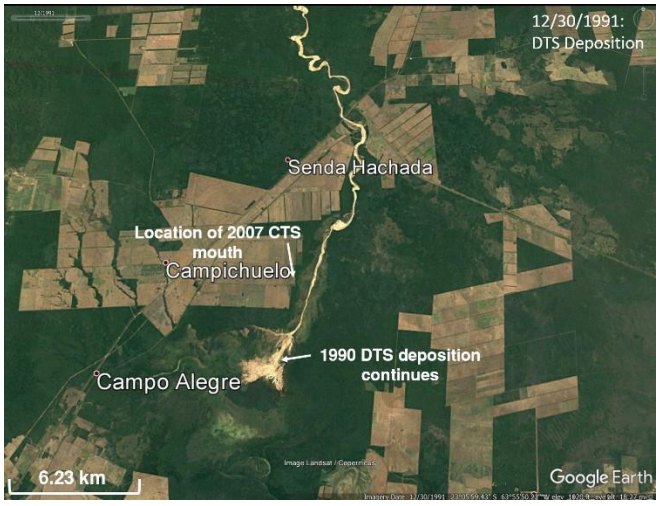

Figure 3.6 Aerial photograph of the terminal splay complex, 12/30/1991 (Google Earth).

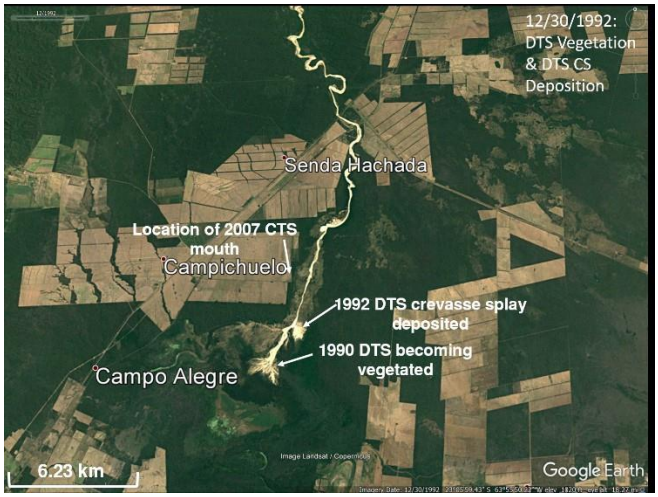

Figure 3.7 Aerial photograph of the terminal splay complex, 12/30/1992 (Google Earth).

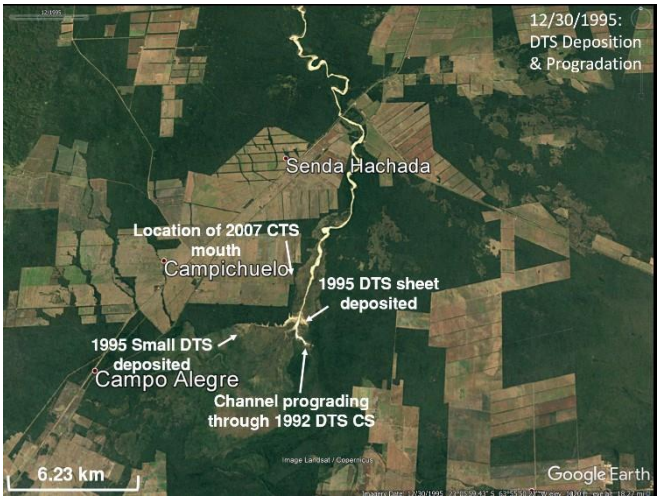

Figure 3.8 Aerial photograph of the terminal splay complex, 12/30/1995 (Google Earth).

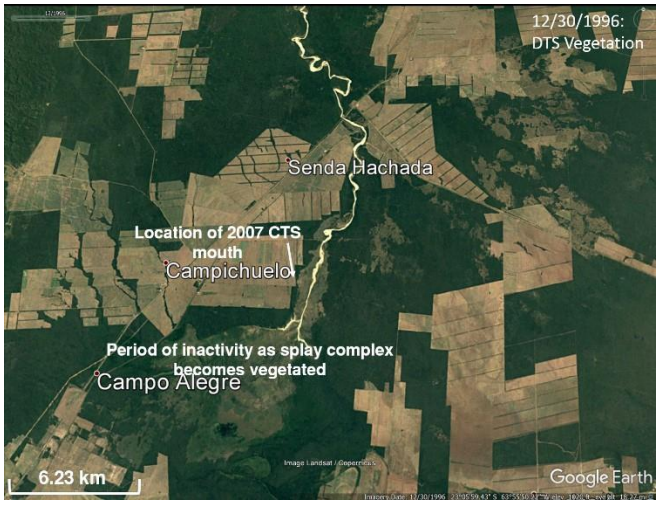

Figure 3.9 Aerial photograph of the terminal splay complex, 12/30/1996 (Google Earth).

Figure 3.10 Aerial photograph of the terminal splay complex, 12/30/1997 (Google Earth).

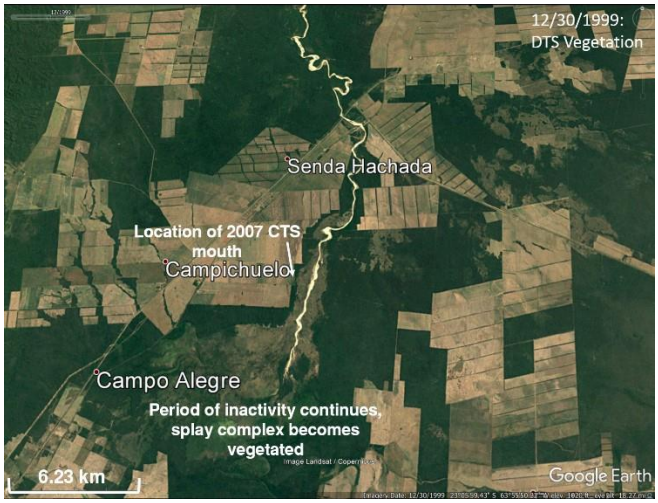

Figure 3.11 Aerial photograph of the terminal splay complex, 12/30/1999 (Google Earth).

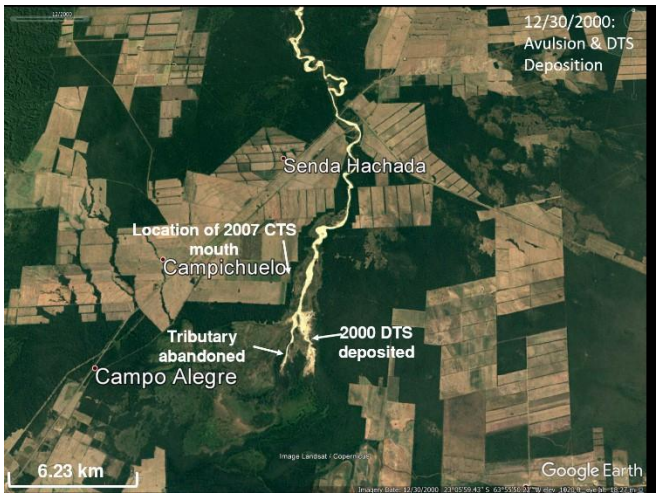

Figure 3.12 Aerial photograph of the terminal splay complex, 12/30/2000 (Google Earth).

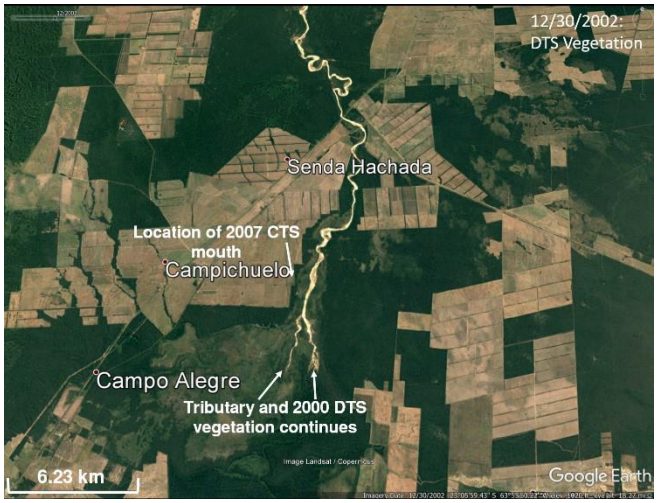

Figure 3.13 Aerial photograph of the terminal splay complex, 12/30/2002 (Google Earth).

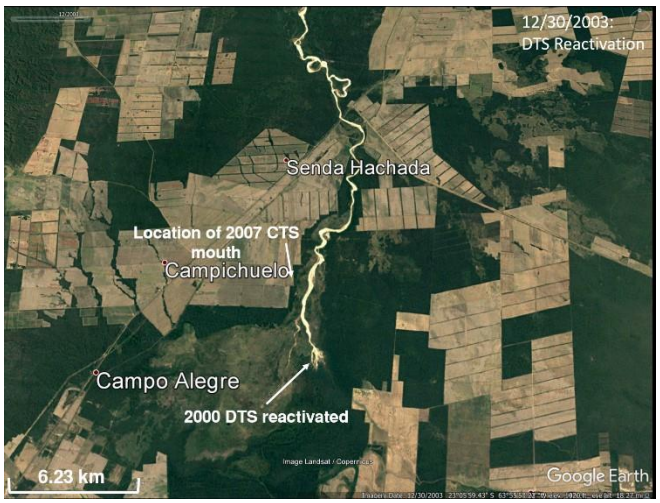

Figure 3.14 Aerial photograph of the terminal splay complex, 12/30/2003 (Google Earth).

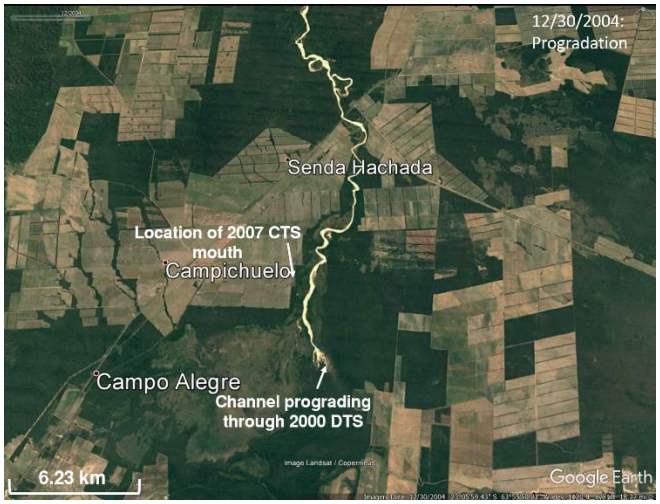

Figure 3.15 Aerial photograph of the terminal splay complex, 12/30/2004 (Google Earth).

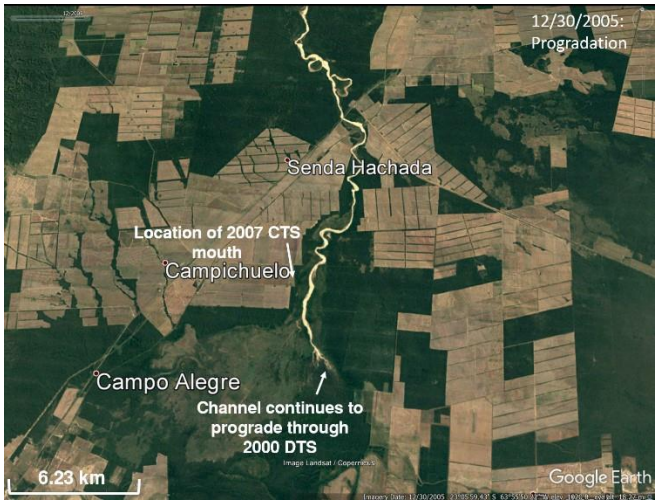

Figure 3.16 Aerial photograph of the terminal splay complex, 12/30/2005 (Google Earth).

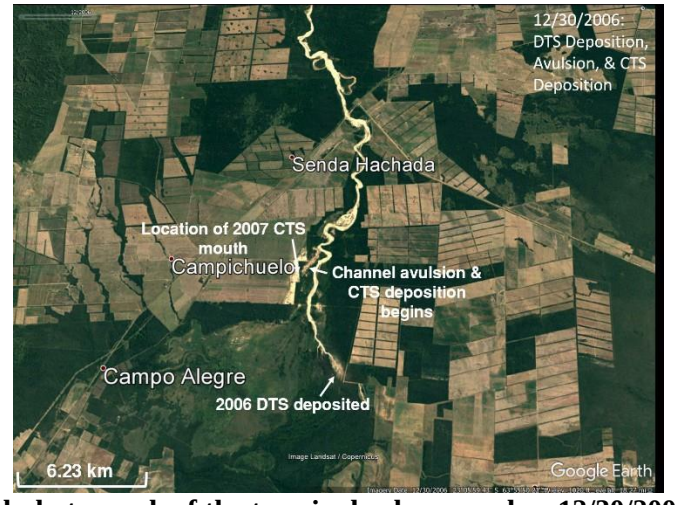

Figure 3.17 Aerial photograph of the terminal splay complex, 12/30/2006 (Google Earth).

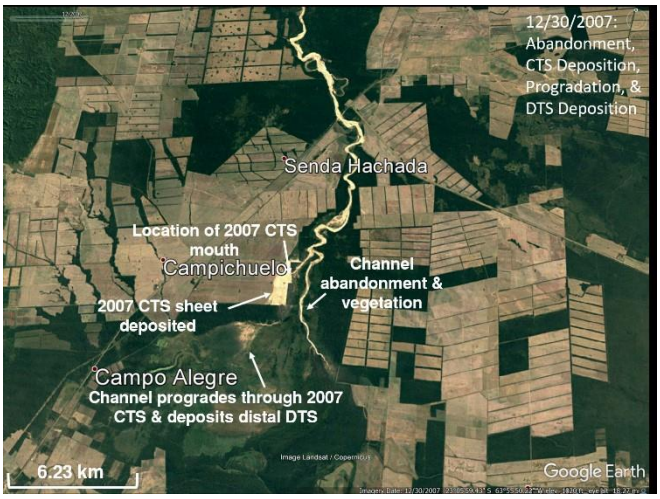

Figure 3.18 Aerial photograph of the terminal splay complex, 12/30/2007 (Google Earth).

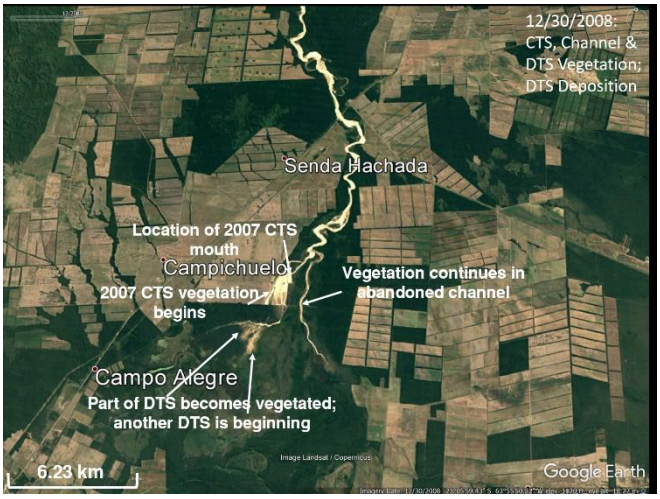

Figure 3.19 Aerial photograph of the terminal splay complex, 12/30/2008 (Google Earth).

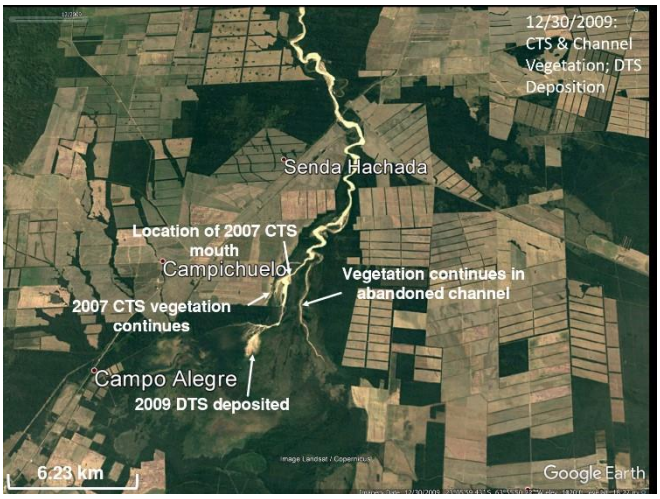

Figure 3.20 Aerial photograph of the terminal splay complex, 12/30/2009 (Google Earth).

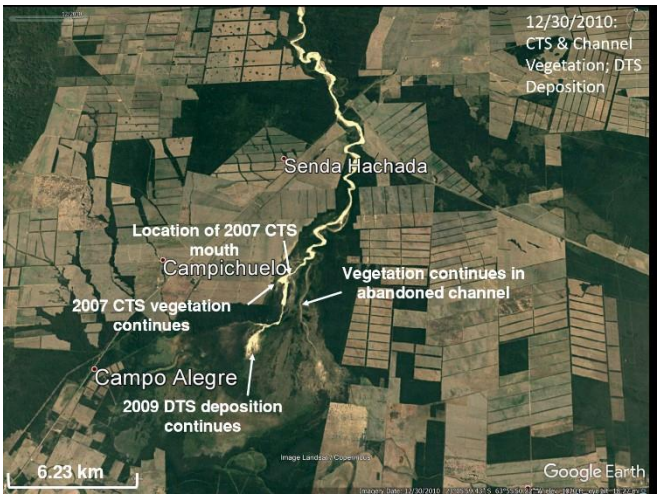

Figure 3.21 Aerial photograph of the terminal splay complex, 12/30/2010 (Google Earth).

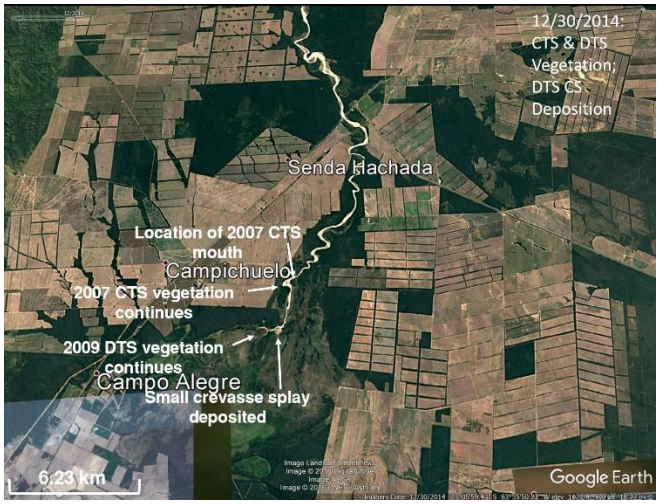

Figure 3.22 Aerial photograph of the terminal splay complex, 12/30/2014 (Google Earth).

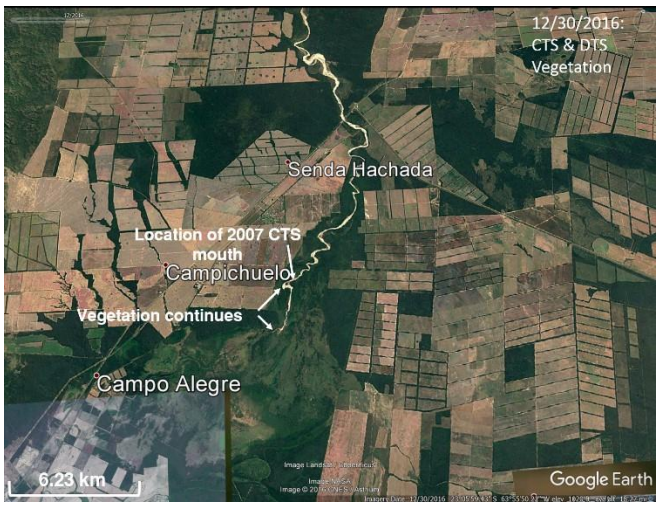

Figure 3.23 Aerial photograph of the terminal splay complex, 12/30/2016 (Google Earth).

In 2007 the Rio Seco deposited a large CTS sand sheet ~1,200 – 1,300 meters wide and ~1,900 meters long (2,375,000 m^2) with lobate form and with mud bypassing down to the Rio Bermejo. As seen on the Google images before and after splay deposition, larger vegetation generally stands. This is further evidenced in the field with upright in-situ trees buried through multiple layers of stacked sand sheets coupled with dendrochronology dating a tree back 20 years. The CTS appears to have recorded one discrete flood event after at least 23 years of non-deposition at the CTS site, whereas the larger DTS complex has grown as discrete avulsing lobes over several intervening and later floods.

III.1.2 Campichuelo Terminal Splay Complex: Facies

III.1.2.1 Terminal Splay Sand Sheet

The terminal splay sand sheet facies comprises loam, very fine – fine loamy quartzose sand, and very fine – fine quartzose sand in fining upward sequences. The grains are well-rounded and well-sorted, and the sand itself is well-sorted. Sand sheet grain size decreases downstream, where sediment is dominated by loam and very fine loamy quartzose sand. Similarly, thickness of the terminal splay decreases downstream. The sedimentary structures within the terminal splay sand sheets are: 1) humpback cross-laminations (*hxl*); 2) planar laminations (*pl*); 3) convex laminations (*cxl*); 4) conventional cross-sets (*cxs*); and 5) backsets (*bs*) terminating up-dip against an upstream erosion surface.

Vegetation is influenced in many ways by the CTS complex, while also having an influence as the complex is re-established. Vegetation of the CTS is dominated by

Yungas moraine forests that quickly grow back between flooding events. While a large amount of vegetation is uprooted or buried during flooding events, some of the larger trees can withstand displacement. Embedded through at least three terminal splay layers of Face 4, a tree was able to stay rooted during the flooding (Figure 3.24). In the distal zone, an in-situ tree survived two splay floodings (Figure 3.25). This tree began to grow following the event that preceded the 2007 CTS. The tree's root system begins at the same level as the silty layer differentiating splay beds and extends down through the top part of the underlying bed.

Figure 3.24 Buried, in-situ tree that survived multiple flooding events. ~1-meter tall.

Figure 3.25 In-situ tree in Face 5. Tree began to grow in between a previous splay and the one deposited in 2007.

III.1.2.2 Intersplay Deposits

Intersplay deposit facies comprise silty clay, silty loam, and very fine – fine quartzose sandy loam. Grain size generally remains consistent throughout with some downstream fining. These sediments are darker in color and tend to have more organic material than the terminal splay and channel fill facies. The silty layers between sand sheets have ~1 cm-thick ripple lamination sets, the only form of sedimentary structures found in this facies. Rooting of surface vegetation extends through these layers, typically churning the interfluve deposits.

III.1.2.3 Channel Deposits

The channel deposit facies contains upper fine-, lower medium-, and medium-grained quartzose sand with limited organics. Flood waters rip up much of the small vegetation, preventing accumulation of organic material. The range of grain sizes can be seen in both upstream and downstream areas of the CTS complex. These sediments are poorly sorted but well rounded. Humback cross-laminations and low angle cross-sets characterize the channel deposit facies. The lensoidal channel deposits possess the same sedimentary structures as the central channel complex, though less persevered due to washout during flooding. Among the channel deposits there is one example of a transverse bar deposits. The bar is characterized by humpback cross-laminations concentrated at different intervals throughout the bed.

III.1.2.4 Flood Basin Mud-Flat (Mollisol)

A flood basin mud-flat deposit with a strong mollic horizon is beneath the splay and channel deposits. This mollic soil horizon is characterized by a dark brown to black clay with abundant organic material (Figure 3.26). Found in 6 different drill-holes throughout the CTS, this horizon serves as a consistent correlative layer representing a period of quiescence where a floodplain clay layer could develop before the terminal splay complex's deposited. Along with floodplain development, vegetation thrived during the period of inactivity, resulting in development of a 1.5 m thick mollic A soil horizon.

Figure 3.26 Sample of the mollisol horizon found throughout the terminal splay complex, abundant with woodchips and other organic material.

III.1.3 Campichuelo Terminal Splay Complex: Architecture

The architecture of the CTS is defined from stream and borehole exposures. The sedimentary structures within the terminal splay complex were studied on 7 different bank exposures along the dried-up river bank (Figure 3.27), with one exposure in the

river bed (Figure 3.29). As aforementioned, the sedimentary structures which make up the sand sheets are: humpback cross-laminations (*hxl*); planar laminations (*pl*); convex laminations (*cxl*) with cross-sets; conventional cross-sets (*cxs*); and backsets (*bs*) (modified after Fielding, 2006). These splays are also excavated in three borehole cross-sections. These cross-sections show the extent, geometry, and stacking of terminal splay sheets and associated facies elements.

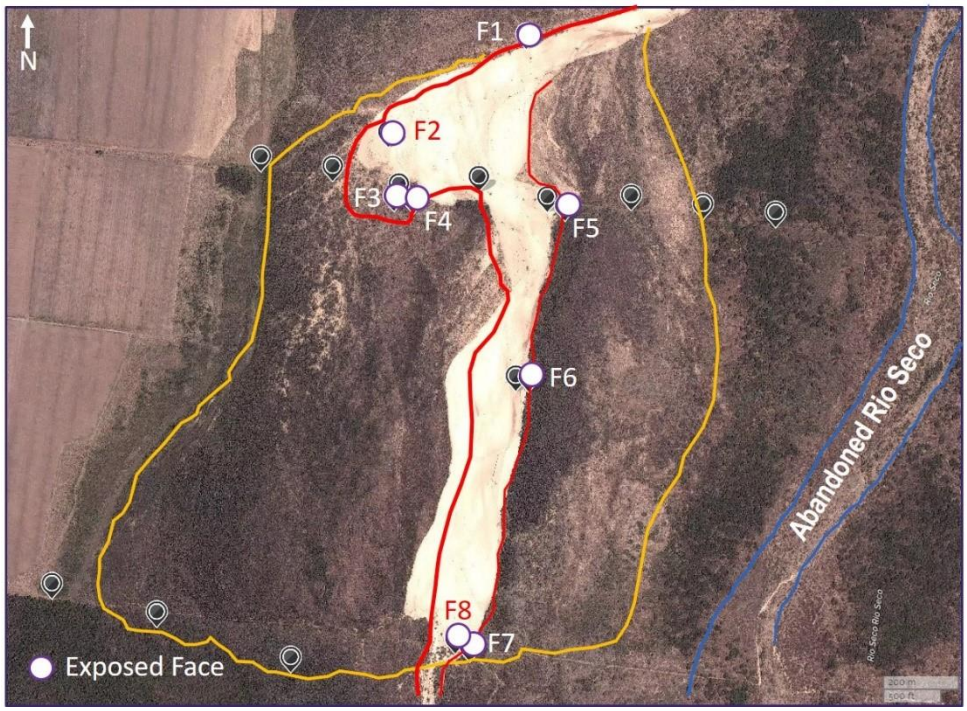

<u>Figure 3.27</u> Campichuelo Terminal Splay complex: location of sedimentary structures studied are indicated by white dots.

Face 1 defines the head of the 2007 CTS and two underlying splays. The three sand sheets in Figure 3.28 all have a silty base, with mixed convex and planar laminations. The top 110-cm-thick bed is the thickest of the splay sand sheets and was deposited during the 2007 CTS flooding event. The bottom third of the 2007 sand sheet has convex laminations (*cxl*) and transitions upward to planar laminations (*pl*). The top half of this splay sheet transitions from humpback cross-laminations (*hxl*) to *pl*.

Underlying the 2007 sand sheet, sheet A is 35 cm-thick beginning with *cxl* that transitions into *pl* and back to *cxl* capping the splay beneath a thin generically sigmoidal layer of silt. Sheet B (55 cm) is dominated by *cxl* with low angle cross-bedding and symmetrical drapes that are located at the base.

	Humpback cross-laminations (*hxl*)
	Planar laminations (*pl*)
	Convex laminations with cross-sets (*cxl*)
	Conventional cross-sets (*cxs*)
	Backsets terminating up-dip against an upstream erosion surface (*bs*)
	Channel lag/mud drapes

Table 3.1 Sedimentary structures within the terminal splay complex.

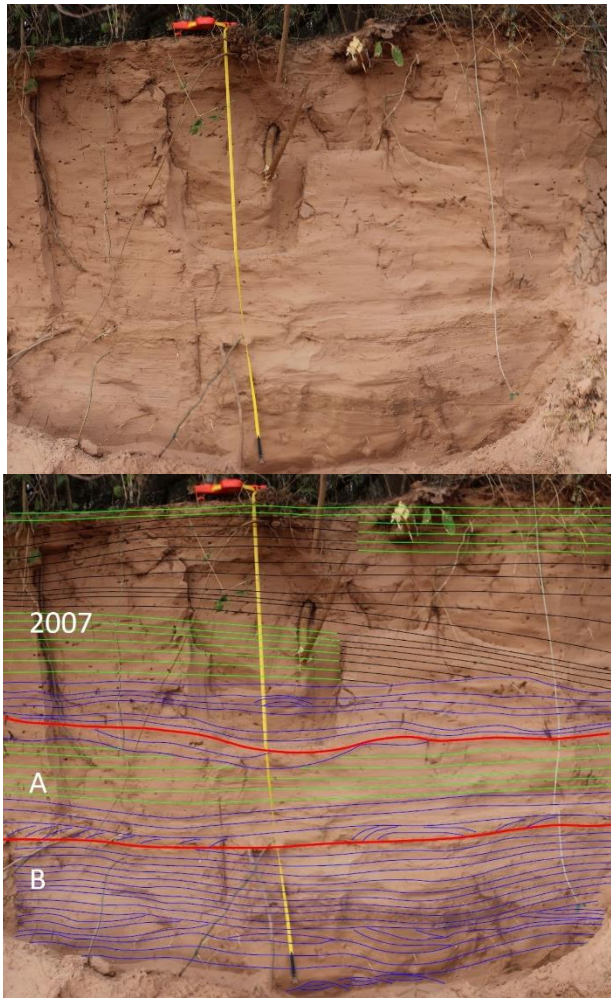

<u>Figure 3.28</u> Face 1 located at the mouth of the terminal splay complex. This face is oriented along dip, photo facing west. Flow is right to left.

Face 2 and 3 (Figure 3.29; 3.30) and 4 and 5 (Figure 3.31; 3.32) are located slightly down dip from the 2007 CTS head and record strike (2 and 3) and dip (4 and 5) orientation. Face 2 is exposed at a bend in the Rio Seco oriented along depositional strike but lacks the 2007 CTS deposit. This face has three sand sheet beds with one containing a small channel incision. Sheet C transitions from *hxl* to *pl* to *cxl*. The transition in sheet C is broken by a thin layer of generically sigmoidal bedding capping the deposit. The base of sheet B transitions from *pl* to *hxl*, both of which are incised by a lensoidal channel that is characterized by convex laminations with cross-sets. Sheet A continues with the trend of *cxl*.

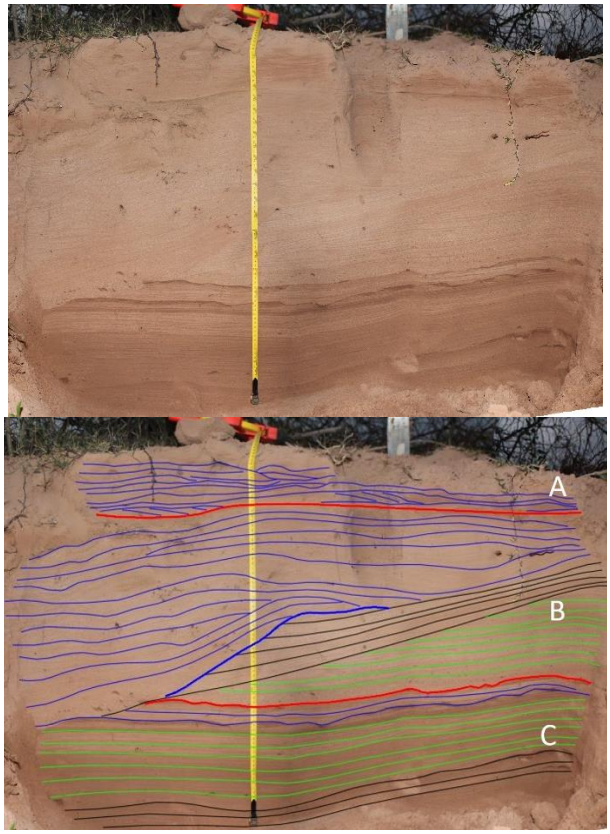

Figure 3.29 Face 2 located in the proximal zone of the terminal splay complex. This face is along strike, photo facing upstream. Flow comes around a bend in the channel from right to left.

Face 3 (Figure 3.30) is oriented along strike in the proximal zone, and is one of two CTS deposit exposures oriented along strike. The 2007 splay is only 27 cm-thick. This sheet is made of solely convex laminations. Sheet A is 42 cm-thick, and the bottom of the sheet is dominated by *cxl* that transitions up into planar laminations. Sheet B (44 cm-thick) also transitions from *cxl* into *pl* bedding, only this sheet goes through at least two cycles and also contains an interval of backsets. Sheet C (50 cm-thick) does not have a defining silt layer indicating its base, and is dominated by humpback cross laminations (*hxl*).

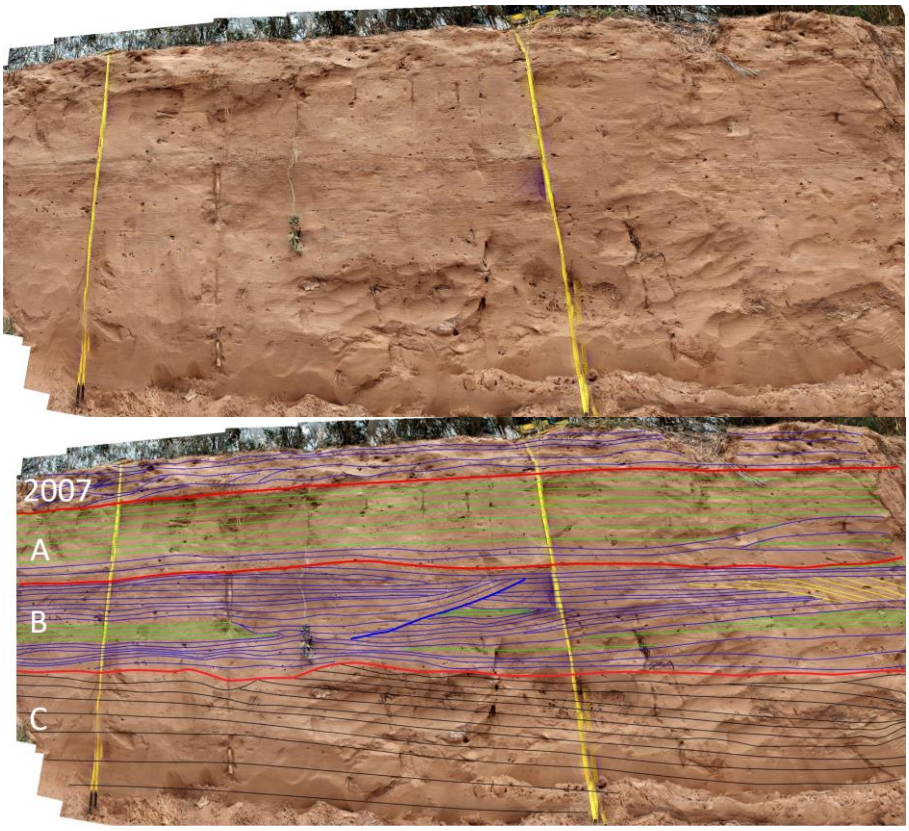

Figure 3.30 Face 3 located in the proximal zone of the terminal splay complex. This face is along strike, photo facing south. Flow is right to left.

Moving from Face 4 (Figure 3.31) to Face 5 (Figure 3.32) from east to west, the sand sheets transition from parallel and planar bedding to convex laminations with cross-sets, respectively. Face 4 has five different sand sheet packages, including the 2007 CTS deposit. This 2007 CTS bed is 45 cm-thick and exhibits convex laminations that transition to planar laminations. Sheets A (53 cm), B (20 cm), C (35 cm) and D (50 cm) are composed dominantly of planar laminations. Sheet C exhibits some conventional cross-sets (CXS) within the planar laminations. The bottom third of sheet D is highlighted by humpback cross-laminations. Face 5 (Figure 3.32) has three thick sand sheet deposits, all containing humpback cross-laminations. The 2007 CTS bed here contains conventional cross-sets in the middle of the 106 cm-thick layer. Sheet A is 80

cm-thick and sheet B is 72 cm-thick. Additionally, the in-situ tree served as an obstacle accumulating debris at its base.

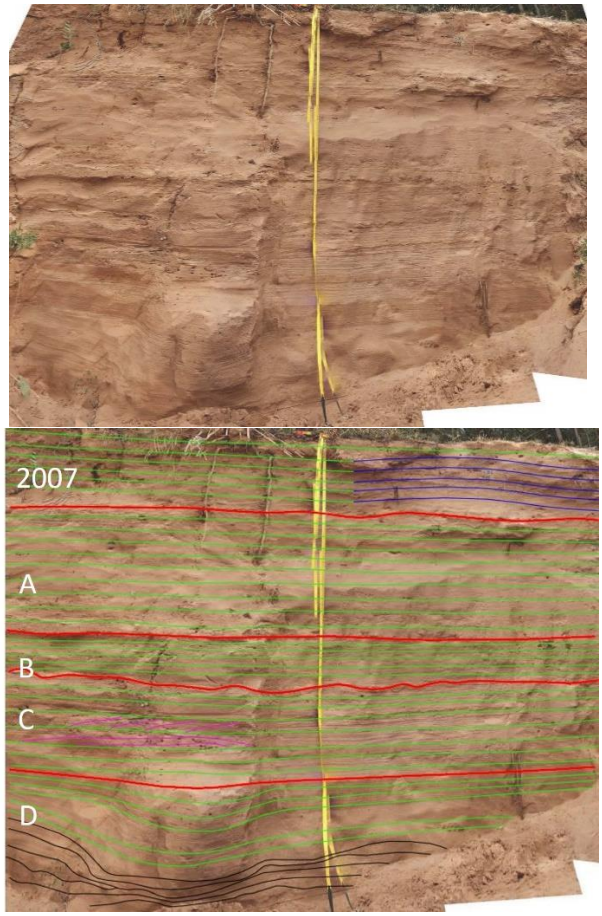

Figure 3.31 Face 4 located in the proximal zone of the terminal splay complex. This face is along dip, photo facing east. Flow is right to left.

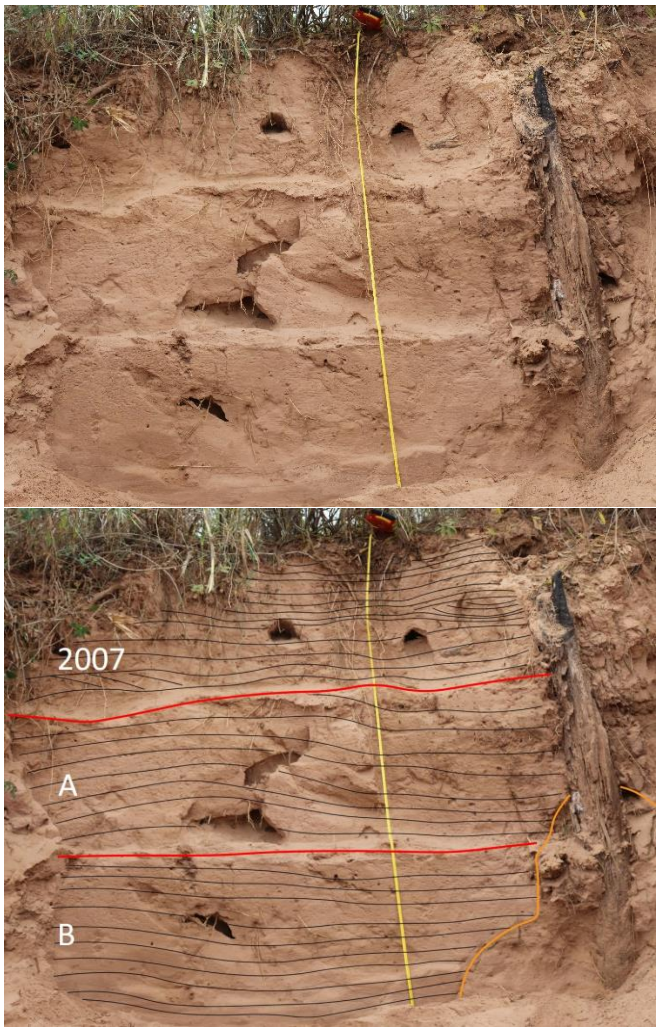

<u>Figure 3.32</u> Face 5 located in the proximal zone of the terminal splay complex. This face is along dip, photo facing east. Debris highlighted in orange. Flow is left to right.

In the medial zone of the CTS (Face 6; Figure 3.33), the 2007 CTS deposit is 35 cm-thick and is characterized by convex laminations with some low angle cross-sets. The underlying 50 cm-thick sheet A contains planar laminations. The three underlying sheets (B, C, and D) are dominated by convex laminations with cross-sets. Sheets B, C, and D are 17, 10, and 33 cm-thick, respectively.

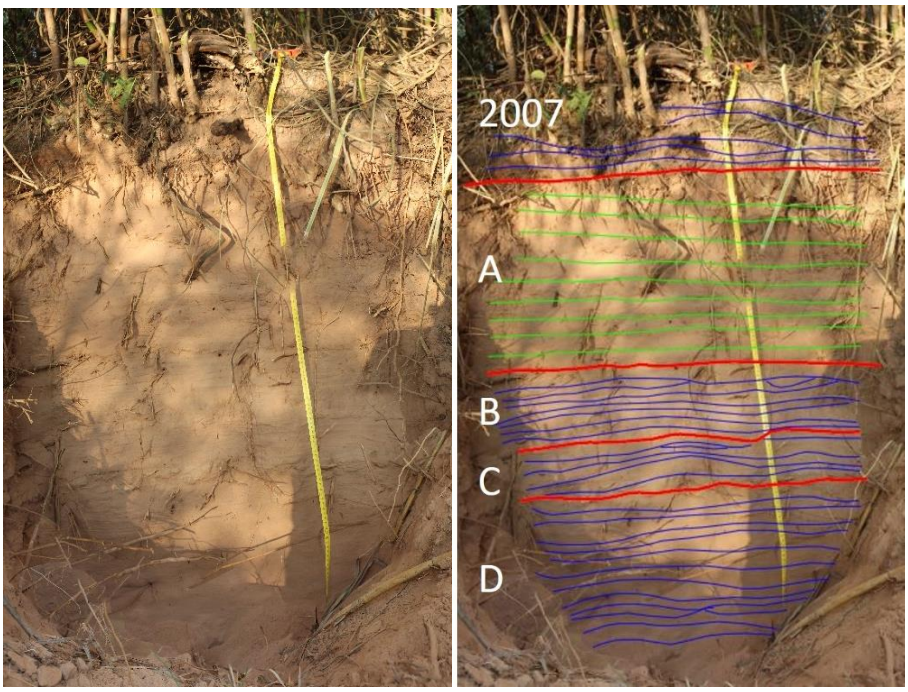

Figure 3.33 Face 6 located in the medial zone of the terminal splay complex. This face is along dip, photo facing east. Flow is left to right.

Exposures in the distal zone include a dip-oriented stacked terminal splay sand sheets (Face 7; Figure 3.34) and an adjacent exposed bar in the channel (Figure 3.35). The 2007 CTS sand sheet in Face 5 is 22 cm-thick containing convex laminations with cross-sets (*cxl*). Sheets A (19 cm), B (28 cm), and C (30 cm) are characterized by *hxl*. Sheet D (20 cm) is covered. Sheet E (50 cm) contains a small channel incision dominated by convex laminations with cross-sets. Below the channel deposit are humpback cross-laminations that transitions up into *cxl* and planar laminations.

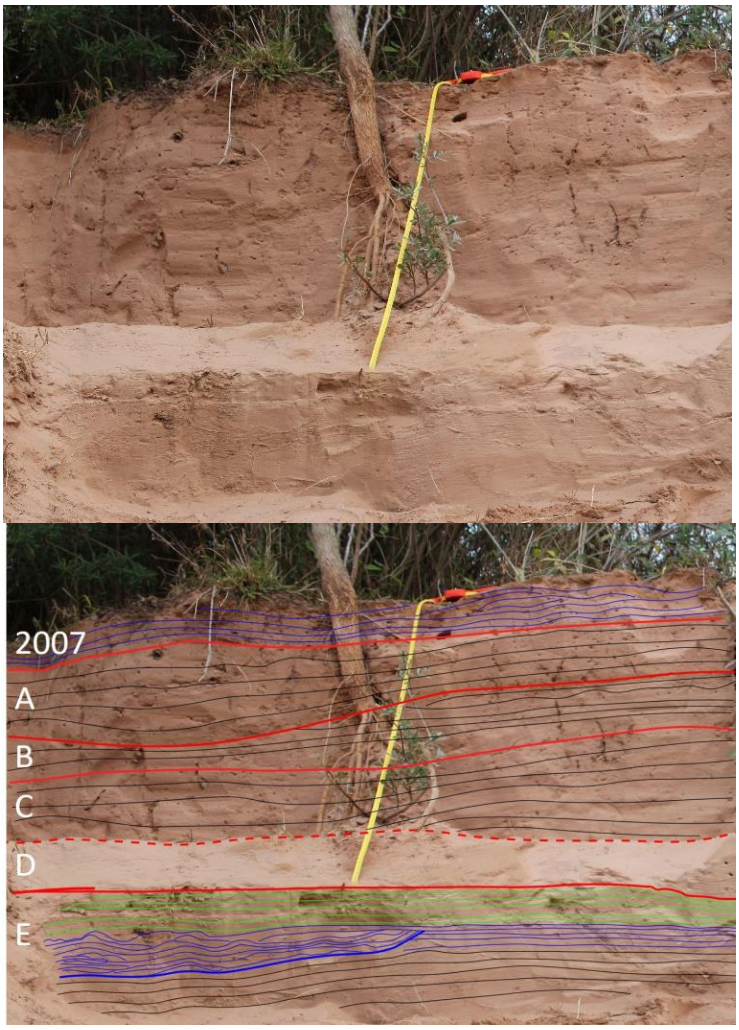

Figure 3.34 Face 7 located in the distal zone of the terminal splay complex. This face is along strike, photo facing south. Flow is left to right.

The face of the transverse bar deposited (Figure 3.35) across the tributary is facing north. The base of the bar exhibits *hxl* and is capped by a generically sigmoidal silty layer. As deposition ensued, several mud drapes were deposited at the base followed by convex laminations with cross-sets. Antidune cross-laminations within the bar are climbing the lee face of the bar and the bar deposit is capped by convex and planar laminations, along with backsets (*bs*) terminating updip against. The bar grew in multiple flow events recorded by differing flow conditions and/or changing flow conditions over

the same flow, as recorded by changing sedimentary structures on the downstream bar accretion face.

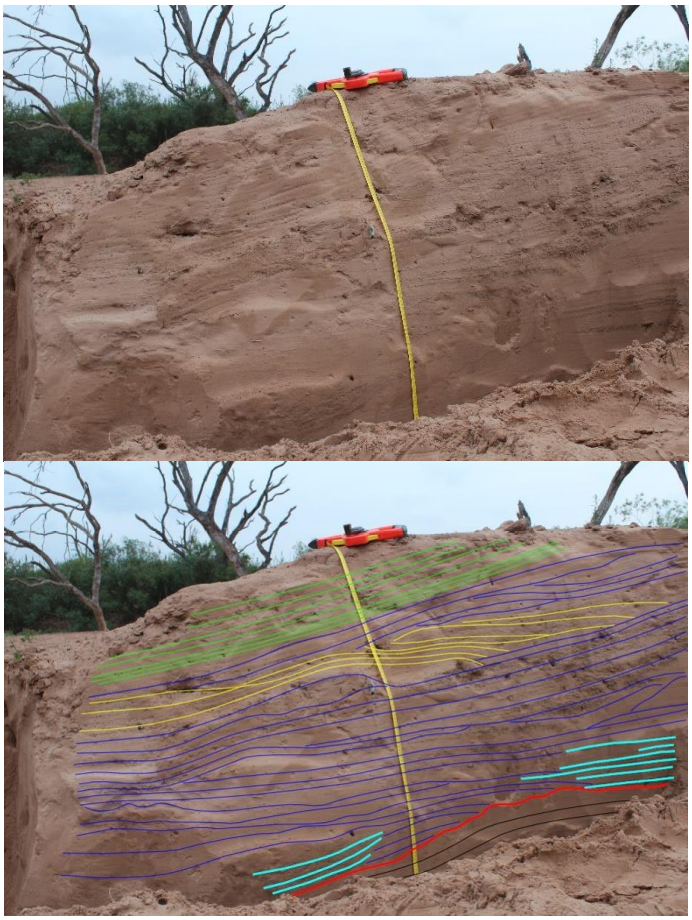

Figure 3.35 Face 8 located in the distal zone of the terminal splay complex. This face is along strike, photo facing south.

The 2007 CTS reaches widths of ~1,200 meters and ~1,300 meters in the proximal and distal zones, respectively. The average thickness of all sand sheets exposed along the river bed is 42.9 cm, compared to an average of 58.5 cm thickness of subsurface sand sheets. Based on drill-hole data, the proximal zone intersplay facies ranges from 20 – 50 cm thick and 20 – 100 cm in the distal zone. Channel deposits in the proximal and distal zones are 90 – 100 cm and 1 – 2 meters thick, respectively. The 2007 CTS sand sheet has an average thickness of 57.5 cm, ranging from 22 – 110 cm. The

volume of sand deposited during the 2007 CTS is ~1.4 million cubic meters over anarea of ~2.37 million square meters. There are up to five exposed sand sheets underlying the 2007 sheet: A (42.0 cm average), B (36.9 cm avg), C (31.2 cm avg), D (34.3 cm avg), and E (50 cm).

Cross-section A-A' defines 9 discrete splays. The mollisol horizon is found in 5 drill-holes along A-A' (Figure 3.36), serving as a consistent correlative basal marker. The sand sheets are stacked on top of each other locally with a relatively thick layer (20 – 50 cm) of intersplay lithofacies. Otherwise, the CTS sand sheets are broken up by thin layers of loam or defined by fining upward sequences. These terminal splay sand sheets have extensive lateral continuity despite their downstream thinning. Channel facies have migrated laterally over time incising pre-existing CTS deposits, with flow mainly occurring through the center of A-A'. In 2009 (Figure 3.20), splays A through E were incised shortly after the deposition of the 2007 CTS as the Rio Seco avulsed into the vicinity of the CTS.

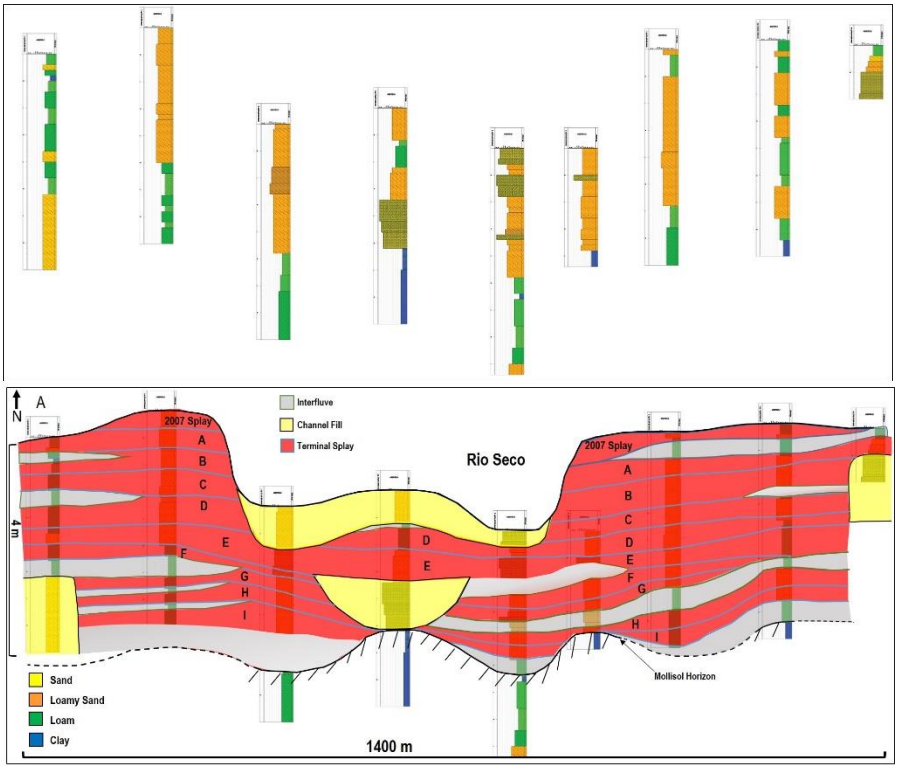

Figure 3.36 Cross-section A-A': Proximal zone of the CTS complex.

Cross-section B-B' (Figure 3.37) illustrates the downstream thinning of splays A – E, including the 2007 CTS deposit. The mollisol horizon that served as a basal marker in cross-section A-A' is identified in 2 drill-holes along this cross-section. The distal zone of the CTS also has flat, laterally continuous sand beds, but the intersplay layers are more continuous than in A-A'. Channel deposit location remains relatively consistent, with the modern channel migrating slightly east downstream.

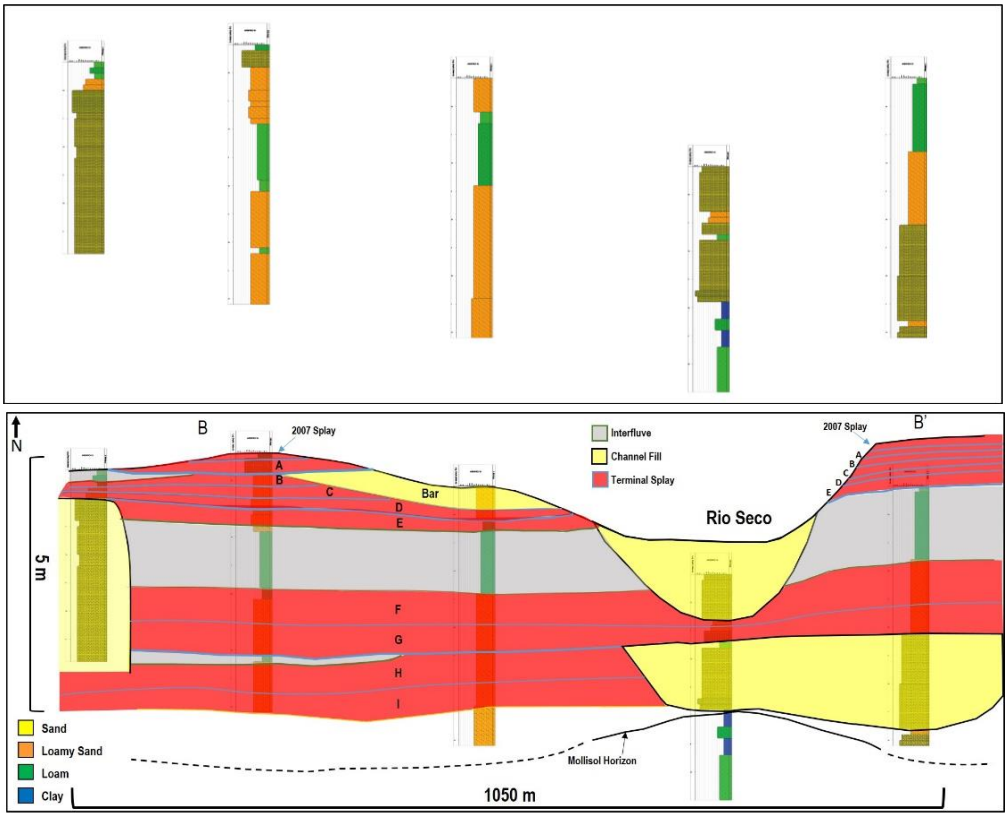

Figure 3.37 Cross-section B-B': Distal zone of the CTS complex.

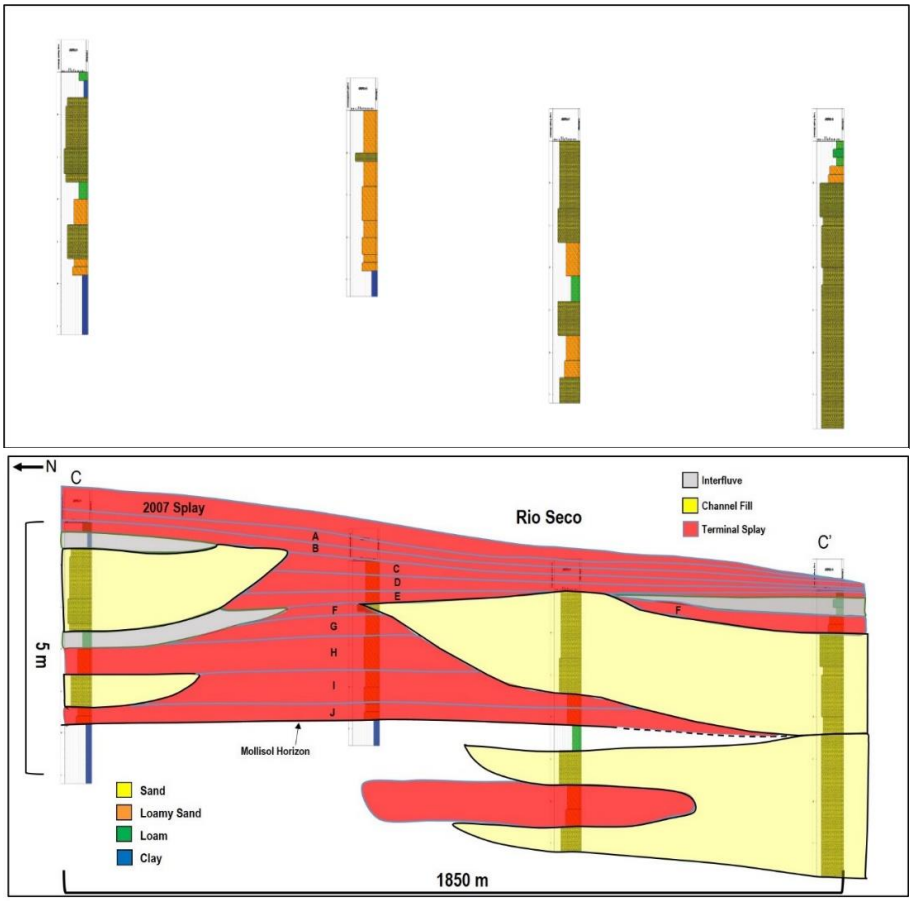

Figure 3.38 Cross-section C-C': Longitudinal profile of the CTS complex.

The 2007 CTS is 57.5 cm-thick on average with a range of 22 – 110 cm. The thickest bed (110 cm) is located at the apex of the splay (Figure 3.28) and thins downstream. At a bend in the channel in the proximal zone, the face oriented along strike (Figure 3.30) is significantly thinner (27 cm) than the two located along dip (Figures 3.31 and 3.32). Moving east the 2007 sheet thickens from 27 cm to 45 cm to 106 cm, an average of 59.3 cm in the proximal zone. The medial zone follows the downstream thinning trend down to 35 cm (Figure 3.33), followed by the thinnest of all, a 22 cm-thick distal splay sheet (Figure 3.34). Similarly, the 2007 CTS sheet's sedimentary structure transitions downstream. At the mouth of the splay, the base is mad of flat, low angle bedding with some convex-upward character with the top two-thirds being parallel and

planar laminations. In the proximal zone, two of the three sheets are FLA dominant and the third is strictly parallel and planar laminations. The medial and distal zone exhibit the transition into humpback cross-laminations. Among other downstream trends, grain size remains very fine with increasing silt content downstream.

III.1.4 Campichuelo Terminal Splay Complex: Vegetation

Flooding plays a major impact on surrounding vegetation. Larger vegetation such as trees are commonly able to withstand flooding and become buried by sediment (Figure 3.39). This is not always true, as some trees and other debris are uprooted and carried downstream upon flooding in the CTS complex (Figure 3.40).

Figure 3.39 Uprooted tree and other debris carried to the distal zone, influence by flooding event. Located next to Face 7, photo facing southeast. Same tree seen in Figures 3.25 & 3.34.

Figure 3.40 Uprooted tree and other debris influence by flooding event, located next to Face 4. Photo facing southeast.

The buried tree in the proximal zone (Figures 3.24, 3.32, and 3.41) has survived several flooding and depositional burial events. As deposition of the middle terminal splay sheet ended, and before the 2007 CTS deposit, the tree was then burned off at ground level (Figure 3.41). Two additional examples of burnt tree stumps were found in the dry river bed (Figures 3.42 and 3.43).

Figure 3.41 Charred cap of the tree embedded in Face 5. Photo facing east.

Figure 3.42 Charred cap of tree stump that was broken off in the dry river bed.

Figure 3.43 Charred cap of tree stump that was broken off in the dry river bed.

Two trees located in the middle of the river bed (Figure 3.44) exhibit sediment stains at approximately the same height that the Figure 3.41 tree was burned off. One of the trees remained intact while the other was snapped off just above the top of the sediment stain and then carried downstream. There are several trees located throughout the river bed, all of which have accumulated debris around their base (Figure 3.45) while the tree serves as an obstacle. The trees in the channel have all been excavated by the Rio Seco after the 2007 avulsion to this site from the level of sediment staining down to the current river-bed level.

Figure 3.44 Downstream view with Face 5 to the left. The two trees in the middle of the stream were stained with sediment up the height that flooding reached.

Figure 3.45 Example of a tree located in the river bed serving as an obstacle, accumulating debris transported downstream.

III.2 Raton Formation Terminal Splay Complex

III.2.1 Raton Formation Terminal Splay Complex: Facies

III.2.1.1 Terminal Splay Sand Sheet

The terminal splay sand sheet facies is characterized by very fine quartzose sandstone sheets that are well-rounded, well-sorted, and slightly silty. The sheets are laterally continuous, with little to no lateral variation in thickness or grain size. These

sand sheets are separated either by intersplay deposits up to 50 cm thick, or locally differentiated by ~1 cm thick layers of muddy siltstone. Sedimentary structures characterizing this facies are: 1) humpback cross-laminations (*hxl*); 2) planar laminations (*pl*); 3) convex laminations (*cxl*) with cross-sets; and 4) conventional cross-sets (*cxs*).

Abundant and well-preserved palm tree trunks (Figure 3.46) and palm fronds (Figure 3.48) are locally embedded within terminal splay sand sheets of the Raton Formation. Tree trunks are commonly preserved upright extending through multiple sheets of sand, commonly with large root-balls at their base (Figure 3.47). The palm fronds and other large vegetation are typically found lying flat at the base of the sand sheets (Figure 3.48). Many of the terminal splay sand sheets are filled with rhizoliths (Figure 3.49) and carbonized roots extending through one or more splay beds.

Figure 3.46 Example of part of a well preserved palm tree trunk within a terminal splay sand sheet.

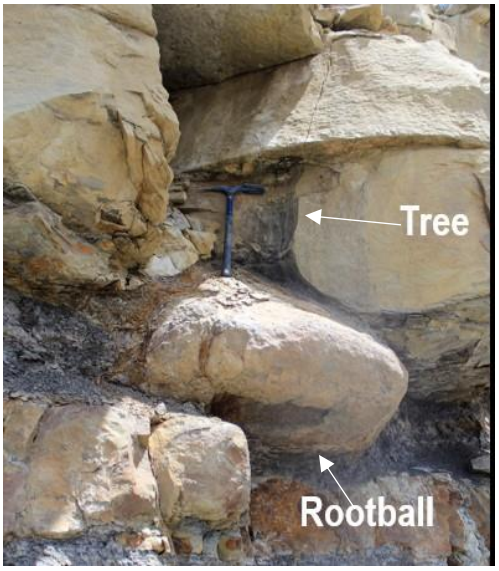

Figure 3.47 Example of part of a well preserved palm tree trunk and the rootball attached to its base (Modified from Horner, 2016).

Figure 3.48 Example of part of a large well preserved palm frond at the base of a terminal splay sand sheet.

Figure 3.49 Example of organic-rich roots (rhizoliths) that grew over the top of a terminal splay sand sheet (Horner, 2016).

III.2.1.2 Intersplay Deposits

The intersplay facies is made up of mudstone, silty mudstone, and muddy siltstone. The intervals composed of mudstone are typically very fissle with abundant organic material like rhizoliths, and small sticks and leaves. The mudstone beds are the thickest of the intersplay facies and makes a slope forming surface. Unlike the typically bulbous silty mudstone, intersplay mudstone is hackly. Silty mudstone layers range from 10 – 20 cm and are filled with larger organic leaves and sticks. Muddy siltstone forms ~1 cm-thick layers breaking up stacked terminal splay sand sheets. The intersplay facies separating the terminal splay sheets are more variable in thickness as well as lithology, but remain laterally consistent.

The intersplay facies preserves smaller leaves, sticks and other organic fragments (Figure 3.50). The smaller organic material found throughout the floodplain deposits can be coaly, and are typically oriented horizontally. Another vegetation feature of intersplay deposits is upright preserved trees and organic root systems. Figure 3.51 shows an intact coalified taproot system which took root atop floodplain deposits. The tree began growth

following intersplay deposition, prior to sand sheet deposition, and was able to survive at least two different splay events.

Figure 3.50 Example of part of a well preserved organic leaf located in the intersplay facies (Horner, 2016).

Figure 3.51 Coalified taproot that grew through intersplay deposits prior to the deposition of the terminal splay sand sheets (Modified from Horner, 2016).

III.2.1.3 Channel Deposits

Large symmetrical channel fill composed of fine-grained sandstone characterize terminal splay complexes in the Raton Formation (Figure 3.52). A 4.8-meter-thick channel sandstone truncates the top of the terminal splay sand sheet and intersplay set near the center, resting right above the flood basin mud-flat coal seams. This channel fill includes low angle ripple laminations that transitioned into parallel and planar laminations, and back to low angle ripples. Among stacked terminal splay sand sheets are lenticular sandstone channel bodies ranging from 12 – 39 cm thick at an average thickness of 28 cm. The lenticular channel bodies are dominated by low angle convex laminations, humpback cross-laminations, and local planar laminations. Unlike the larger central channel fill, the lenticular channel bodies are subject to preservation of small vegetation and rooting on the surface.

III.2.1.4 Flood Basin Mud-Flat and Swamp

The flood basin mud-flat facies is a thick, dark bituminous coal that can be found throughout the Raton Formation. This facies is of interest as it has served as a source for coal bed methane production in the area. The significance of the facies for this study is the relationship to the mollisol horizon found beneath the CTS complex. Both the coal and the mollisol horizons represent a long period of time in which the area saw muddy, organic-rich floodplain deposition opposed to that of a channel. The coal seams of the Raton Formation's terminal splay complex are thick and laterally extensive. This facies differs from the intersplay deposits as it is represented by the long period of fluvial

quiescence prior to the terminal splay complex establishing. The intersplay deposits represent shorter periods of inactivity between splay sheet depositions.

III.2.2 Raton Formation Terminal Splay Complex: Architecture

In the center of the outcrop (Figure 3.52) is a 4.8-meter-thick symmetrical channel fill that cuts into the stacked terminal splay sand sheets and intersplay deposits. The channel fill is flanked on both sides by extensive splays laterally which the channel later cut. In between stacked sand sheets are thin intersplay silt deposits in addition to the larger intersplay packages breaking up splays. Among the stacked terminal splay sheets are lenticular channel bodies that are scattered throughout the terminal splay complex. These sheets are bundled into complexes of sets of splays pierced by channel(s) between thicker muddy abandonment phases for the splay complex. Thickness of the sheets has little variation, with the exception that some beds pinch out. The average thickness of the terminal splay sand sheets is 14.89 cm, ranging from 4 – 35 cm-thick beds. The sand sheets on the east side of the valley fill average a thickness of 14.05 cm compared to 15.72 cm on the west side.

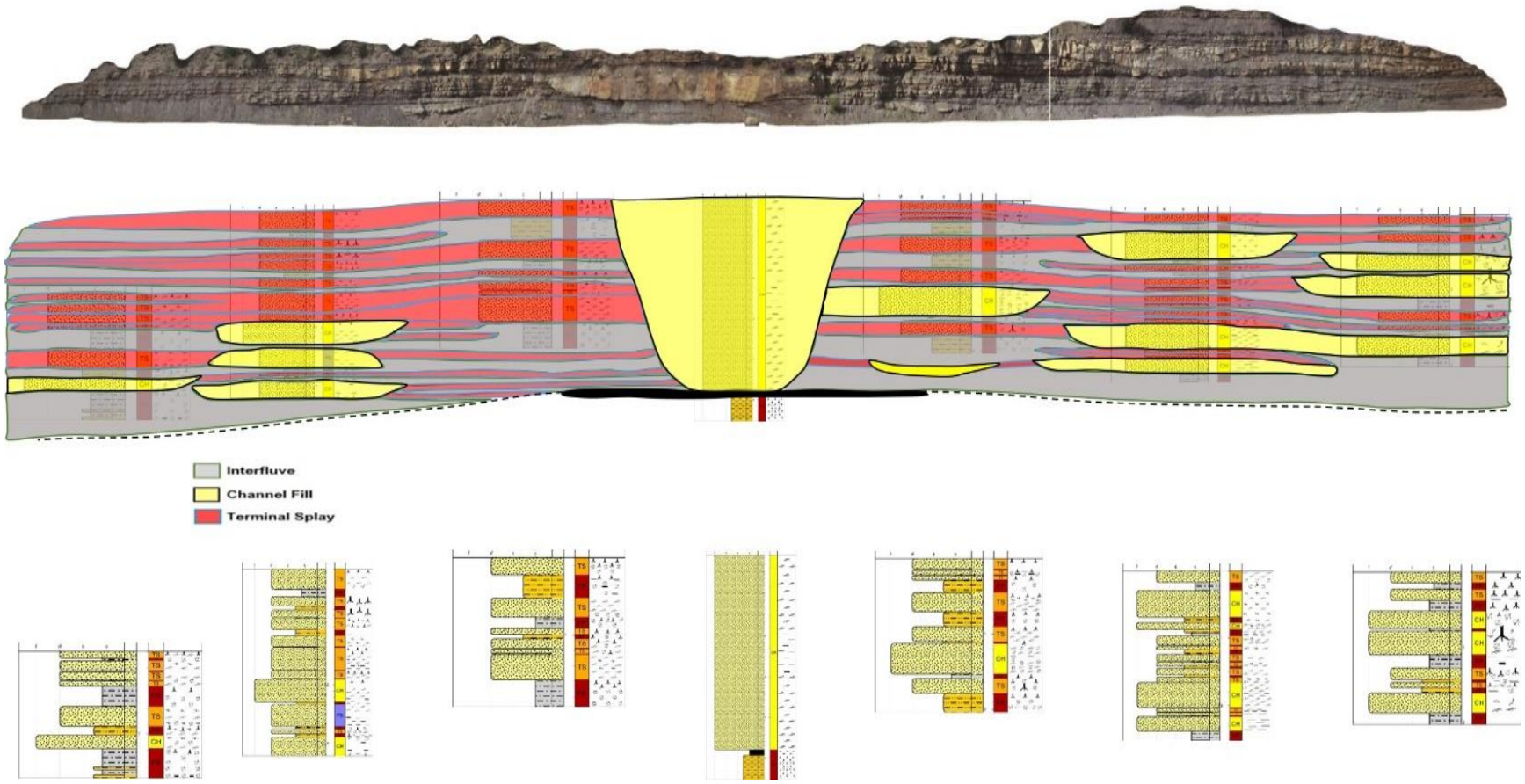

Figure 3.52 Vertically exaggerated Lower Valdez section. Terminal splay sand sheet deposits are red, intersplay deposits grey, and channel fill deposits are yellow.

The terminal splay sand sheets are characterized by low angle convex laminations with cross-sets (*cxl*), planar laminations (*pl*), and low angle humpback cross-laminations (*hxl*); back-sets (*bs*) and conventional cross-sets (*cxs*) are also present. This is based off of 7 measured sections within the Lower Valdez outcrop (Figure 3.53). Of the 33 terminal splay beds, 24 are dominated by low angle convex laminations. Commonly convex laminations pass to planar laminations and transition back into ripple laminations upward, though 2 splay sheets contained strictly planar laminations. Rooting and other vegetation is present in 25 different beds, 9 of which possess no sedimentary structures due to vegetation interaction. Convex laminations with some cross-sets and humpback cross-laminations are common of the channel bodies (Figure 3.54).

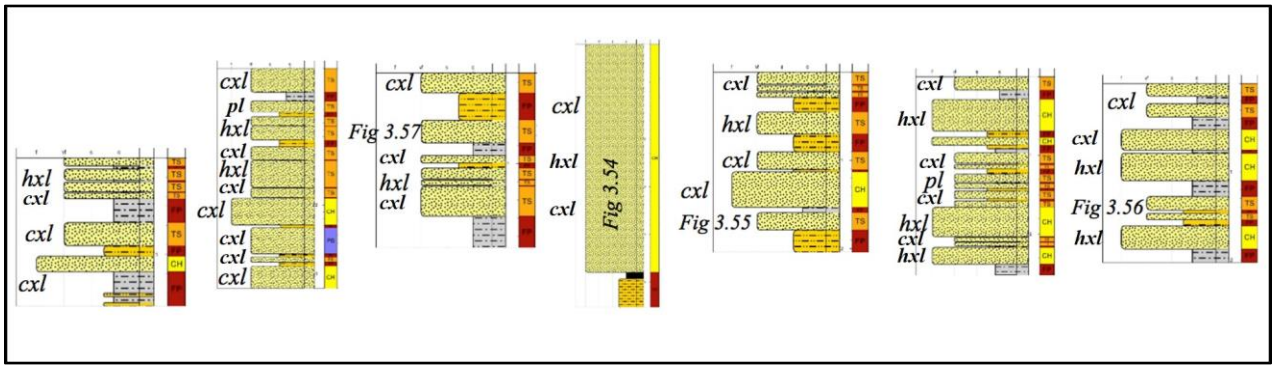

Figure 3.53 Lower Valdez section detailing the sedimentary structures of the terminal splay complex.

Figure 3.54 Channel deposit. Convex laminations with cross-sets and humpback cross-laminations.

Convex laminations with cross-sets are also dominant in terminal splay sand sheets and can contain back-sets (Figure 3.55). Planar laminations are not as common in the Raton Formation's terminal splay sand sheets, but they do exist. Planar laminations tend to transition into humpback cross-laminations (Figure 3.56), a feature seen in Argentina terminal splay sheets. Humpback cross-laminations are also common among the Raton Formation (Figure 3.57). While they can transition into planar laminations, they oftentimes stand alone and are laterally continuous.

Figure 3.55 Terminal splay sand sheet. Convex laminations with conventional cross-sets and back-sets.

Figure 3.56 Terminal splay sand sheet. Convex laminations with conventional cross-sets and back-sets.

Figure 3.57 Terminal splay sand sheet. Humpback cross-laminations.

IV. Discussion

IV.1 Comparison of CTS and Raton Terminal Splay Complexes

Architecture of the two terminal splay complexes is similar. Cross-sectional views in A-A' and the Lower Valdez outcrop are both (Figure 4.1) characterized first by a large central channel complex that cut and filled multiple times. Extending like wings off the side of the large channel fills are laterally continuous terminal splay sand sheets. Sand sheet thickness has little variation laterally until near termination in both locations. A longitudinal section is available for the CTS complex and here splays thin downstream. The splay sheets in both systems commonly extend beyond the current exposure but also are incised by small channel deposits or pinch out. As splay sand sheets further from the main channel body they may exhibit slumping. The intersplay deposits between sand sheets in both examples are analogous. Intersplay deposits are thin where flooding occurs in quick

succession. During that brief period, only a thin layer of silt deposits between splay sand sheets. This is the case for most of the exposed faces of the CTS and many splays in the Raton Formation.

The terminal splay sand sheets deposited in both analogs are composed of very-fine quartzose sand that is well sorted and well rounded. The Raton splay sheets are slightly silty compared to the CTS' clean sand sheets. Based on sedimentary structures, flow regime is also similar between the two basins. Both of these systems are indicative of a high flow regime, a very important similarity when comparing the two. Vegetation interaction in the terminal splay complexes is another striking commonality. Humid terminal splay complexes transition from flooded sandy areas to being completely vegetated in a short period of time.

Although the depositional orientation of the Lower Valdez outcrop is uncertain, it is nearly or completely a strike section based on geometry of splays and channels and orientation of sedimentary structures. It is ~350 meters wide and approximately one quarter smaller than the CTS complex. Similarly, the Raton Formation's terminal splay sand sheets are much thinner than those in the CTS complex (Figure 3.52). The river system that formed the Raton splay complex exposed in the Lower Valdez outcrop was considerably smaller than the Rio Seco system.

IV.2 Terminal Splay Complex Depositional Processes

The Rio Seco avulsed into this area in 2007 and the splays beneath record when the Rio Seco made a splay complex here sometime before the 1980's. The mollisol predates that and is of a date unknown. It records a long period predating the terminal splay complex

over top of which the 2007 splay is part. The thick coal seam and surrounding mudstone at the base of the Raton Formation terminal splay complex represents a similar process. Before the splay complex began deposition, this location was a stagnant and swampy environment with abundant organics accumulating to form this thick accumulation of flood-basin deposits in the Raton Formation. Available imagery dates as far back as 1984, but the Campichuelo Terminal Splay complex began much earlier. The standing trees excavated by the Rio Seco appear rooted in the mollisol beneath the splay complex based on excavation at Face 4 (Figure 3.44), thus deposition of the splay complex was sufficiently recent to permit preservation of these trees.

As the Rio Seco loses gradient, the very fine sand grains moving as bedload deposited in a sheet-flow over the vegetated floodplain as a terminal splay. The suspended load continued down flow with the water discharge into the Rio Bermejo. Following the 2007 CTS' deposition, the Rio Seco prograded to the southern terminal splay complex. As a result, the channel cuts down ~2 m through four terminal splay sand sheets. The same process appears to characterize the Raton Formation terminal splay complex. The large channel fill deposit has been cut and filled numerous times as the channel body prograded and incised through the complex while depositing sheet flows and accumulating flood plain sediment.

The terminal splay sheets in Argentina show fluctuation of flow regimes with a dominance of upper flow regime structures. The trend of convex laminations with cross-sets changing to planar laminations is common during deposition. On many of the exposed splay faces, the base of the terminal splay sand sheets begin with low angle convex laminations with some cross-sets. Fielding (2007) identified this as recording flow

transitioning from the upper plane bed to the antidunal bedform stability field. Before the antidunal stability field is reached and flow begins to decrease, planar laminations are indicative of a down step in flow regime to upper plane bed forms. The downstream trend in the sedimentary structures in splays is evidence of flow slowing during deposition. Upon flooding, the channel flows swiftly forming antidunes and swaley beds until flow begins to wane and goes back down to the upper plane bed. The Raton terminal splay sand sheets exhibit nearly all of the same sedimentary structures as the CTS, vertically and along strike, though the dip similarities cannot be confirmed. Terminal splay sand sheets in both analogs are dominated by planar laminations and convex with cross-sets. Splay boundaries in both are indicated by swaley silty layers. Additionally, humpback cross-laminations are common but not dominant in both analogs.

Vegetation interaction is one of the most intriguing similarities between the two systems. Intersplay floodplain deposits are dense with small chips and fragments of sticks and leaves. This organic rich material can be coaly in both analogs, and plant material is well preserved in the Raton Formation. Following terminal splay sand sheet deposition, grass, trees, and other vegetation establish root systems extending through the sand, often disrupting the sedimentary structures. Once the vegetation takes root, it can extend through several splay deposits. The rootlets in the CTS become organic rhyzoliths like those of the Raton Formation (Figure 3.49). Similar to their roots, tree trunks are commonly preserved vertically through several beds of splay and interfluve deposits in both the Raton and CTS systems.

The flow regime in these systems can be very powerful, to the point where whole trees are transported downstream to the distal zone of the terminal splay complex. There

are several instances of trees preserved horizontally oriented in the Raton Formation, but for the most part the trees were vertical in life position. These same trends are in the Campichuelo Terminal Splay. Within the river bed there is a large amount of trees, smaller vegetation and debris lying down, but the surrounding area is heavily wooded. In both analogs the tree's root system lie atop an interfluve deposit. During the period of quiescence the tree continues growth and by the next flooding event it is well secured to withstand the flow. Some CTS trees extend vertically through as much as 5 meters of sediment and 9 splays and are rooted in the basal mollisol horizon (Figure 3.32). This compares to Raton Formation trees (Figure 3.51) with root systems extending down and tree trunks holding firm through successive splay sheets (Figure 3.46). At the same height which the buried tree was broken, these two trees were stained brown from the 2007 event, indicating the maximum height that the channel rose. The same trend can be seen in the Raton as trees vary on how many beds they extend through. The interval at which trees root and brake also varies in both systems. Some CTS trees root in the basal mollisol and extend up through all splays (Figure 3.32), but others root in higher splays and extend upward through successive splays (Figure 3.34). This trend of rooting at multiple horizons and extending through splays above is evident in the Raton Formation as well (Figure 3.51). Fires also commonly burn trees extending above the surface and are the reason trunks do not extend through successive layers (Figure 3.32).

As the base of a terminal splay complex, the organic rich mollisol horizon formed prior to the complex's development. This thick and organic rich bed represents a flood plain during a period of fluvial quiescence. Upon initial progradation the Rio Seco locally incised the mollisol horizon and left buried channel deposits. Similarly the thick Raton coal

seams underlying the splay complex is partly incised by large channel fill deposits (Figure 3.52). Repeated flooding causes transecting channels to cut and fill repeatedly.

Terminal splay systems can migrate as well. The CTS was preceded by another larger terminal splay complex ~1,000 meters south. The Rio Seco migrates the splay systems from the large terminal splay complex back to the CTS and back down south again. As a result of tributary migration, splay complexes can become abandoned for long periods allowing for inter complex deposits like the mollisol horizon to develop. This abandonment period can be at the scale of splays, resulting in intersplay deposits, or at the scale of splay complexes, resulting in thicker flood basin sections, respectively.

The terminal splay complexes in the Raton Formation and Campichuelo shared many characteristics in common (Figure 4.1). First, both were deposited in a humid/tropical depositional environment based on common dominance of humid subtropical vegetation. Splay sheets in both fluvial systems are upper flow regime as evidenced by sedimentary structures indicative of upper plane bed, antidunal stability field, and the transition between the two. The fluctuation of terminal splay sand sheet deposition during flooding and intersplay deposition during quiescent periods provides the splay – intersplay stacking patterns observed in both analogs. While stacking occurs on the flanks on the channel, the channel itself is continually incised and dissects the splay complex. Both also have vegetative structures recording rapid burial of foresets by splay sheets followed by a reestablishment of vegetation. The terminal splay complex in the Raton Formation is characteristic of the terminal end of a DFS like in the Campichuelo Terminal Splay complex. Figure 4.1 illustrates several similarities of the two complexes.

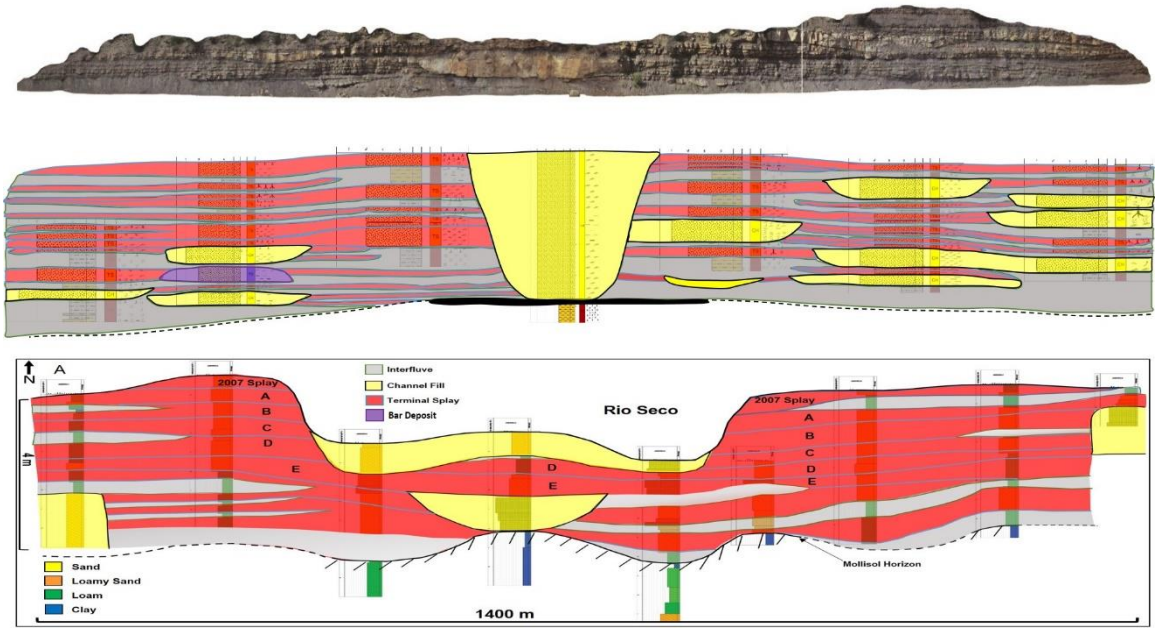

Figure 4.1 Cross-sectional comparison of the Raton Formation's terminal splay complex and the Campichuelo Terminal Splay complex. Top two sections represent the Raton, where the bottom represents the CTS.

IV.3 Implications for Petroleum Extraction

Terminal splay complexes have great potential as hydrocarbon reservoirs. The organic rich flood basin mud-flat facies serves as the main petroleum source of the system with some help from organic intersplay deposits. The intersplay deposits are also seals above and below the terminal splay sand sheets. The dissected channel fill is the most promising reservoir, but the flaking terminal splay sand sheets could provide additional resources to the channel. Though thin, the splay sheets are very extensive and clean. The 2007 CTS splay for instance is ~1,250 m wide, 1,900 m long, and an average of 57.5 cm thick and includes ~1.4 million cubic meters of clean sand. Aspect ratios of thickness to width of splay sheets are on the order of 1:1000. Splay sheets are connected by the incising channel. When extracting petroleum from the channel fill, sand sheets bounded by intersplay seals will funnel any existing hydrocarbons to the channel fill. This is aided by

the geometry of the flanking sand sheets' downward slumping character, creating a stratigraphic trap in the channel fill. The key for success is the lateral connectivity of the terminal splay sand sheets along with the truncating channel fill, which in turn makes all of the sand bodies in these complexes become a single reservoir.

V. Conclusions

Terminal splay complexes are deposited by a distributive fluvial system for the Raton Formation and Rio Seco systems. Terminal splay sheets are thin, very fine-grained sand bodies, though the Raton tended to be siltier. Splay sheets in both complexes are dominated by convex laminations with cross-sets and planar laminations, bound above and below by a thin shale or mudstone. The Raton terminal splay sand sheets exhibit nearly all of the same sedimentary structures as the CTS, vertically and laterally. Despite not having insight to downstream trends or variation, I propose that the same processes have occurred in the Raton Formation.

Another key similarity is geometry. Like the Rio Seco, the Raton Formation exposure is a stacked sequence of terminal splay sand sheets interbedded with intersplay floodplain deposits, incised by a prograding channel of fine-upper fine clean sand. Both examples are incised near the middle of the terminal splay complex. Additionally, the mollisol horizon of the Campichuelo Terminal Splay complex and the large coal seam are correlative. Both of these deposits were formed during periods of little to no fluvial activity in a swampy, organic rich environment. The coal beds of the Raton Basin are heavily explored, and I believe the mollisol horizon comes with the same potential. These organic rich beds also have potential to serve as a source to the surrounding terminal splay sheets

and channel deposits. If there are terminal splay sheets deposited below the coal and mollisol, they can also serve as a seal for migrating hydrocarbons.

The abundance and similarities of the complexes' vegetation cannot be ignored. The fossilized tree trunks and root systems can be linked directly to the large trees of the CTS complex. The fossilized tree trunks can often extend through multiple layers, but is almost always truncated by an overlying terminal splay sand sheet. This is explained in the CTS on the proximal face with an in-situ tree. I propose this tree, and the adjacent trees in the middle of the river bed, took root in the mollisol decades ago. This strong foundation allows the trees to withstand flooding and burial over many years. Eventually, the trees in the river bed will too be buried and preserved in terminal splay sand sheets. Likewise, the smaller rootlets growing into sand sheets will be preserved as organic-rich rhizoliths. Vegetation is functionally the biggest difference between humid and arid terminal splay systerms.

References

Baltz, E.H. (1965). Stratigraphy and history of Raton Basin and notes on San Luis Basin, Colorado-New Mexico. *Bulletin of the American Association of Petroleum Geologists, 49* (11), 2041 – 2075.

Billingsley, L.T. (1977). *Stratigraphy of the Trinidad Sandstone and associated Formations, Walsenburg area, Colorado*. Paper presented at the Symposium on exploration frontiers of the central and southern Rockies: Rocky Mtn. Assoc. Geologists.

Billingsley, L.T. (1978). Stratigraphy of the Pierre Shale, Trinidad Sandstone, and Vermejo Formation, Walsenburg area, Colorado – a deltaic model for sandstone and coal deposition; in Hodgson, H.E., ed., Proceedings of the Second Symposium on the Geology of Rocky Mountain Coal: Colorado Geological Survey, Resource Series 4, p. 23 – 24.

Blakey, R.C. (2014). Paleogeography and Paleotectonics of the Western Interior Seaway, Jurassic – Cretaceous of North America. *AAPG Search and Discovery Article 30392,* p. 1 – 72.

Chace, C.G., Sussman, A.J., and Coblentz, D.D. (2009). Curved Andes: goid, forebulge, and flexure: Lithosphere, v. 1, p. 358 – 363.

DeCelles, P.G. (2012). Foreland basin systems revisited: variations in response to tectonic settings, in Busby, C., and Azor Pérez, A., eds., Tectonics of Sedimentary Basins: Recent Advances: Blackwell Publishing, p. 405 – 426.

DeCelles, P.G. and Giles, K.A. (1996). Foreland basin systems. *Basin Res.,* 8, 105 – 123.

Fielding, C.R. (2006). "Upper flow regime sheets, lenses and scour fills: Extending the range of architectural elements for fluvial sediment bodies." *Papers in the Earth and Atmospheric Sciences.* Paper 296.

Fisher, J.A., Krapf, C.B.E., Lang, S.C., Nichols, G.J. and Payenberg, T.H.D. (2008). Sedimentology and architecture of the Douglas Creek terminal splay, Lake Eyre, central Australia. *Sedimentology, 55(6),* 1915–1930.

Flores, R.M., and Tur, S.M. (1982). Characteristics of deltaic deposits in the Cretaceous Pierre Shale, Trinidad Sandstone, and Vermejo Formation, Raton Basin, Colorado; The Mountain Geologist, v. 19, p. 25 – 40.

Flores, R. M. (1987). Sedimentology of Upper Cretaceous and Tertiary Siliciclastics and Coals in the Raton Basin, New Mexico and Colorado.

Flores, R. M., and Pillmore, C. L. (1987). Tectonic Control on Alluvial Paleoarchitecture of the Cretaceous and Tertiary Raton Basin, Colorado and New Mexico. *Special Publication - Society of Economic Paleontologists and Mineralogists, 39,* 311-320.

Graham, J.R. (1983). Analysis of the Upper Devonian Munster Basin, an example of a fluvial distributary system. In: Collinson, J.D., Lewin, J. (Eds.), Modern and Ancient Fluvial Systems, Special Publication, International Association of Sedimentologists, vol. 6, pp. 473-484.

Hartley, A.J., Weissmann, G.S., Nichols, G.J., Warwick, G.L., (2010). Large Distributive Fluvial Systems: Characteristics, Distribution, and Controls on Development. Journal of Sedimentary Research 80, 67-183.

Hirst, J.P.P. (1991). Variations in alluvial architecture across the Oligo-Miocene Huesca Fluvial System, Ebro Basin, Spain. In: Miall, A.D., Tyler, N. (Eds.), The Three-Dimensional Facies Architecture of Terrigenous Clastic Sediments and its Implications for Hydrocarbon Discovery and Recovery. SEPM (Society for Sedimentary Geology) Concepts in Sedimentology and Palaeontology, vol. 3, pp. 111-121.

Horner, R.J., McGregor, G.E., and Holbrook, J.M. (2017). Vegetation induced sedimentary structures and fossilized trees in terminal splay sandstone beds of the Cretaceous – Paleocene Raton Formation, Colorado. Geological Society of America *Abstracts with Programs.* Vol. 49, No. 2

Horner, R. J. (2016). Facies characterization and architectural context of terminal splay sandstone beds in the cretaceous-paleocene raton formation, colorado (Order No. 10250078). Available from Dissertations & Theses @ Texas Christian University; ProQuest Dissertations & Theses Global.

Horton, B.K. and DeCelles, P.G. (1997). The modern foreland basin system adjacent to the central Andes. *Geology,* 25, 895 – 898.

Johnson, R.C., and Finn, T.M. (2001). Potential for a basin-centered gas accumulation in the Raton Basin, Colorado and New Mexico. *U.S. Geological Survey Bulletin.*

Johnson, R.B. and Wood, G.H., Jr. (1956). Stratigraphy of Upper Cretaceous and Tertiary rocks of the Raton basin, Colorado and New Mexico: American Association of Petroleum Geologists Bulletin, v. 40, p. 707 – 721.

Jordan, T.E. (1995). Retroarc foreland and related basins. In: *Tectonics of Sedimentary Basins* (Eds C.J. Busby and R.V. Ingersoll), pp. 331 – 362. Blackwell Science, Cambridge, MA.

Lang, S.C., Payenberg, T.H.D., Reilly, M.R.W., Hicks, T., Benson, J., Kassan, J., (2004). Modern Analogues for Dryland Sandy Fluvial-Lacustrine Deltas and Terminal Splay Reservoirs. *APPEA Journal*, 329-356.

MacCarthy, I.A.J. (1990). Alluvial sedimentation patterns in the Munster Basin, Ireland. *Sedimentology* 37, 685-712.

McGlue, M.M., Smith, P.H., Zani, H., Silva, A., Carrapa, B., Cohen, A.S., and Pepper, M.B., (2016). An Integrated Sedimentary Systems Analysis of the Rio Bermejo (Argentina): Megafan Character in the Overfilled Southern Chaco Foreland Basin. *Journal of Sedimentary Research*, v. 86, p. 1359 – 1377.

Nichols, G.J. (1987). Structural controls on fluvial distributary systems-the Luna System, Northern Spain. In: Ethridge, F.G., Florez, R.M., Harvey, M.D. (Eds.), Recent Developments in Fluvial Sedimentology. Special Publication, vol. 39. Society of Economic Palaeontologists and Mineralogists, pp. 269-277.

Nichols, G.J., and Fisher, J.A. (2007). Processes, facies and architecture of fluvial distributary system deposits. Sedimentary Geology 195, 75-90.

Olson, D.M., Dinerstein, E., Wikramanayake, E.D., Burgess, N.D., Powell, G.V.N., Underwood, E.C., D'Amico, J.A., Itoua, I., Strand, H.E., Morrison, J.C., Loucks, C.J., Allnutt, T.F., Ricketts, T.H., Kura, Y., Lamoreaux, J.F., Wettengel, W.W., Hedao, P., and Kassem, K.R. (2001). Terrestrial ecoregions of the world: a new map of life on Earth: Bioscience, v. 51, p. 933 – 938.

Pillmore, C.L. (1969). Geology and coal deposits of the Raton coal field, Colfax County, New Mexico: Mountain Geologist, v. 6, p. 125-142.

Pillmore, C.L., and Maberry, J.O. (1976). The depositional environment and trace fossils of the Trinidad Sandstone, southern Raton basin, New Mexico: New Mexico Geological Society, Guidebook 27, p. 191 – 195.

Pillmore, C.L., and Flores, R.M. (1987). Stratigraphy and depositional environments of the Cretaceous-Tertiary boundary clay and associated rocks, Raton Basin, New Mexico and Colorado, *in* Fasset, J.E., and Rigby, J.K., Jr., eds., The Cretaceous-Tertiary Boundary in the San Juan and Raton Basins, New Mexico and Colorado: Geologic Society of America Special Paper 209, p. 111-130.

Pillmore, C. L., and Flores, R. M. (1990). Cretaceous and Paleocene Rocks of the Raton Basin, New Mexico and Colorado—Stratigraphic-Environmental Framework. *Guidebook - New Mexico Geological Society, 41*, 333-336.

Sadler, S.P., and Kelly, S.B. (1993). Fluvial processes and cyclicity in terminal fan deposits: an example from the Late Devonian of southwest Ireland. Sedimentary Geology 85, 375-386.

Scott, G.R. and Pillmore, C.L. (1989). Geologic and structure contour maps of the Raton 1/2° x 1° quadrangle, Colfax and Union counties, New Mexico and Las Animas County, Colorado: U.S. Geological Survey, Open-file Report 89-282, scale 1:100,000.

Smith, P., House, J.I., Bustamante, M., Sobocká, J., Harper, R., Pan, G., West, P.C., Clark, J.M., Adhya, T., Rumple, C. (2016). Global change pressures on soils from land use and management. Glob. Chang. Biol. 22, p. 1008 – 1028.

Strum, S.R. (1984). Depositional environments and lithofacies of the Raton Formation, eastern Raton Basin, New Mexico [M.S. thesis]: Raleigh, North Carolina State University, 81 pp.

Varis, O., Biswas, A.K., and Tortajada, C., eds. (2008). Management of transboundary rivers and lakes: Berlin, Springer, p. 304.

Weissmann, G.S., Harley, A.J., Scuderi, L.A., Nichols, G.J., Davidson, S.K., Owen, A., Ghosh, P. (2013). Prograding distributive fluvial systems: geomorphic models and ancient examples. *New Frontiers in Paleopedology and Terrestrial Paleoclimatology: SEPM, Special Publication*, 104, 131 – 147.

APPENDIX

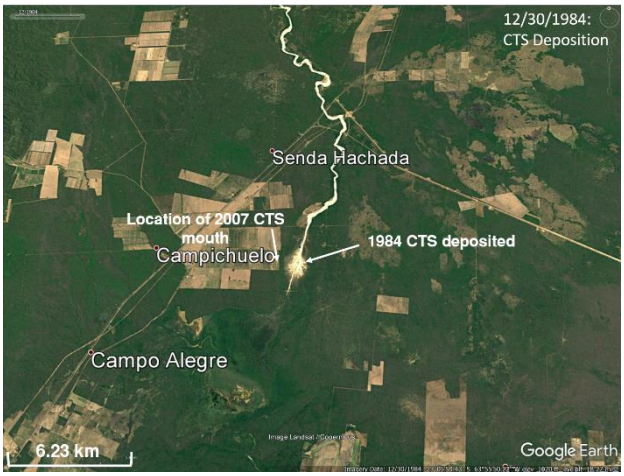

Figure A.1 Aerial photograph of the CTS complex, 12/30/1984 (Google Earth).

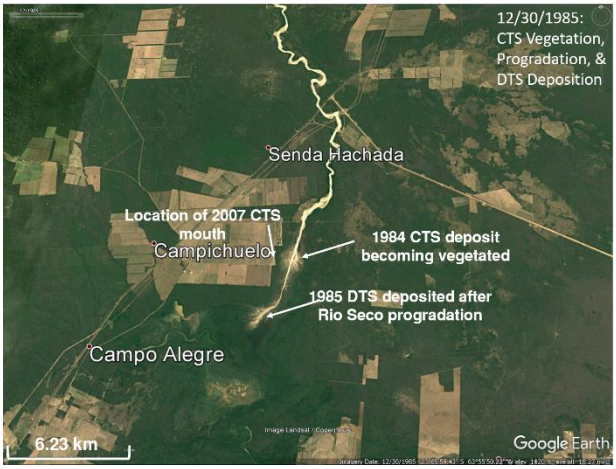

Figure A.2 Aerial photograph of the CTS complex, 12/30/1985 (Google Earth).

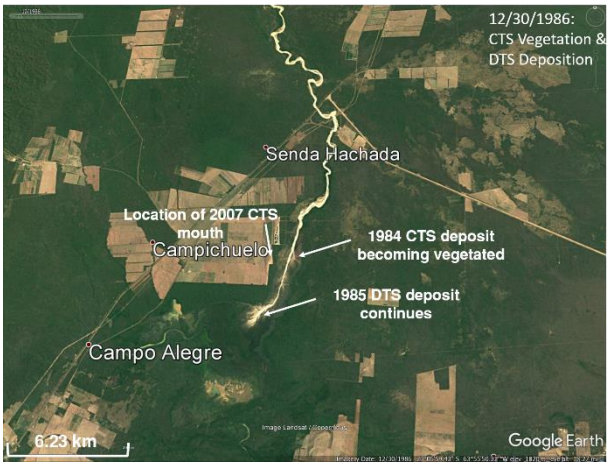

Figure A.3 Aerial photograph of the CTS complex, 12/30/1986 (Google Earth).

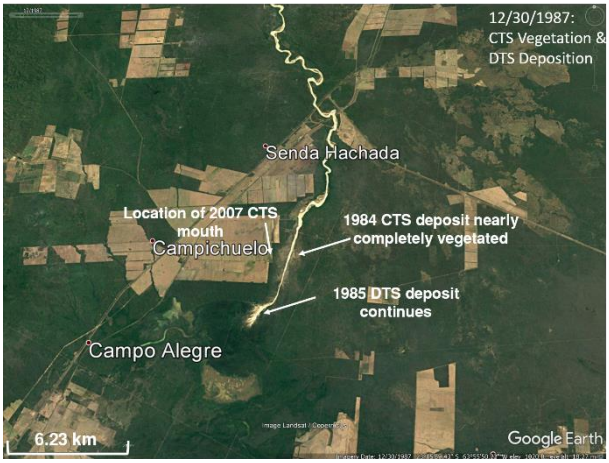

Figure A.4 Aerial photograph of the CTS complex, 12/30/1987 (Google Earth).

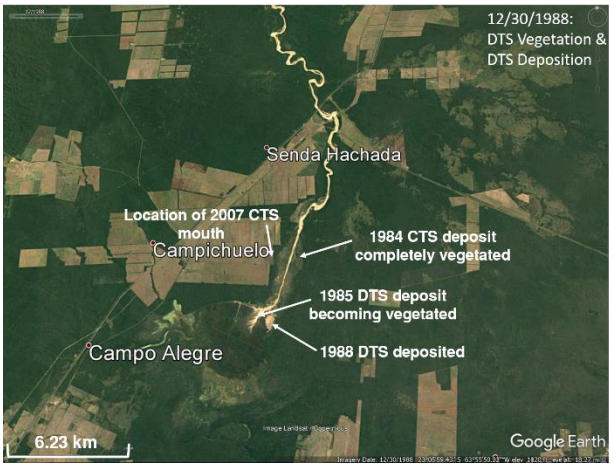

Figure A.5 Aerial photograph of the CTS complex, 12/30/1988 (Google Earth).

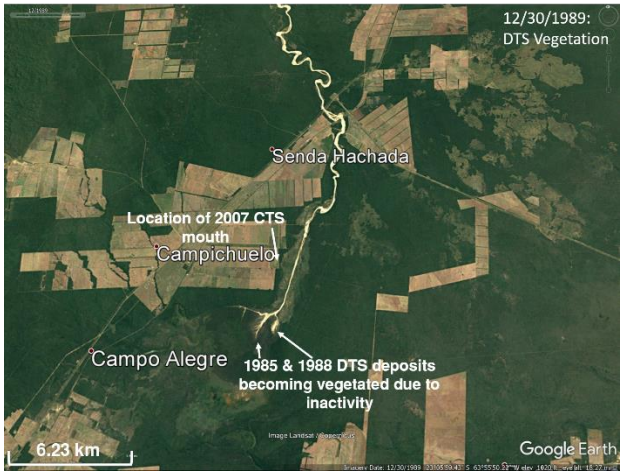

Figure A.6 Aerial photograph of the CTS complex, 12/30/1989 (Google Earth).

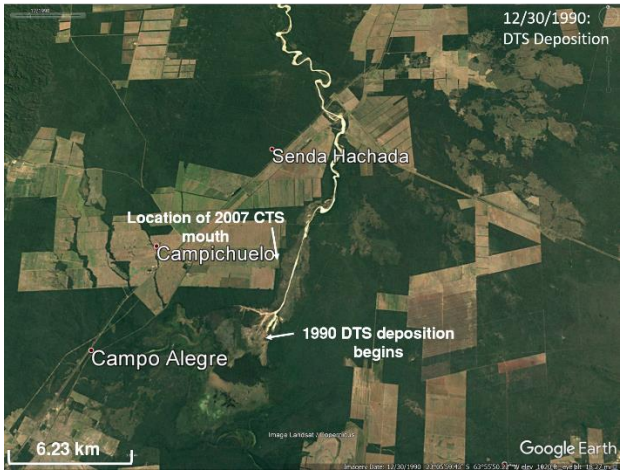

Figure A.7 Aerial photograph of the CTS complex, 12/30/1990 (Google Earth).

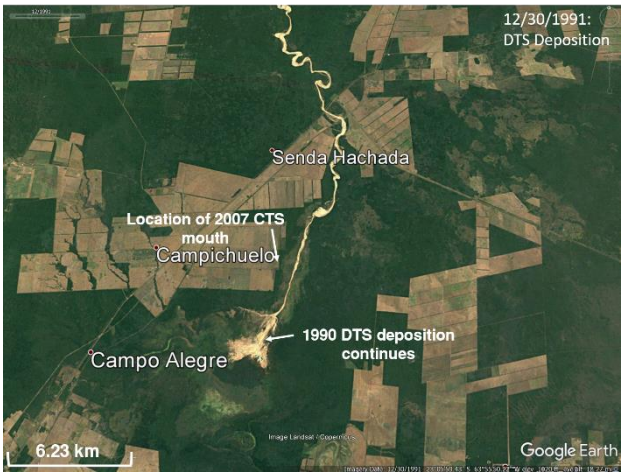

Figure A.8 Aerial photograph of the CTS complex, 12/30/1991 (Google Earth).

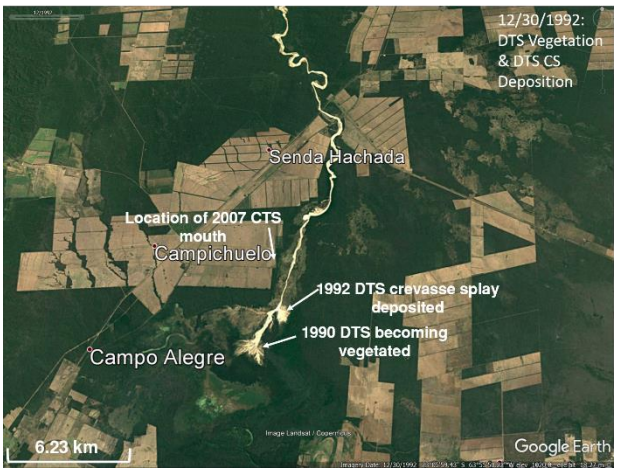

Figure A.9 Aerial photograph of the CTS complex, 12/30/1992 (Google Earth).

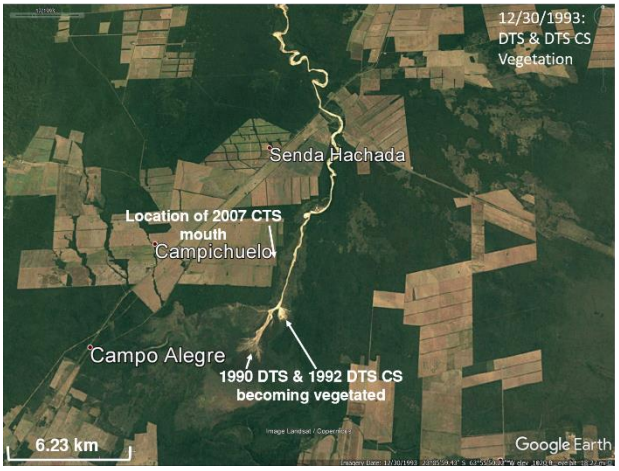

Figure A.10 Aerial photograph of the CTS complex, 12/30/1993 (Google Earth).

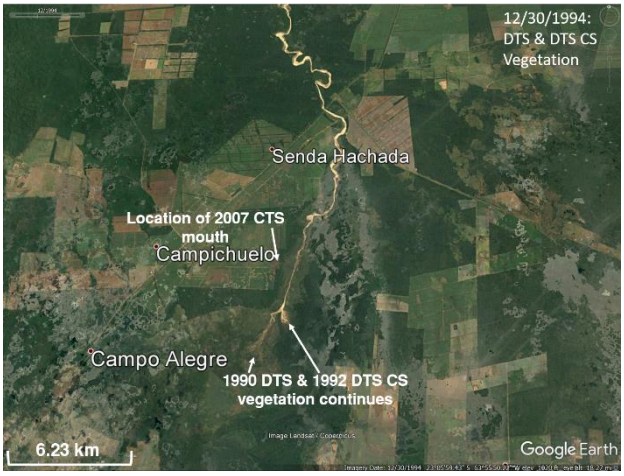

Figure A.11 Aerial photograph of the CTS complex, 12/30/1994 (Google Earth).

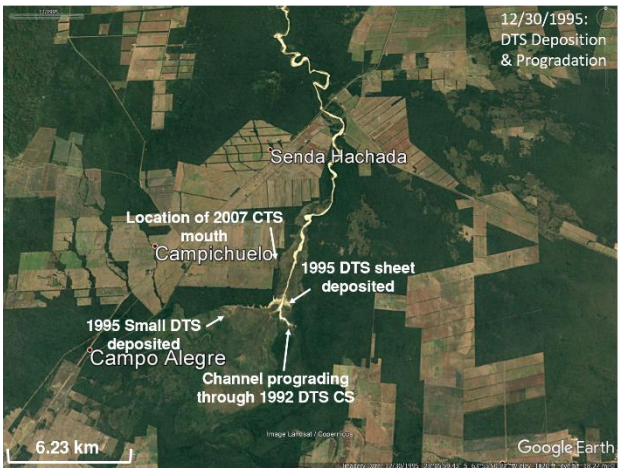

Figure A.12 Aerial photograph of the CTS complex, 12/30/1995 (Google Earth).

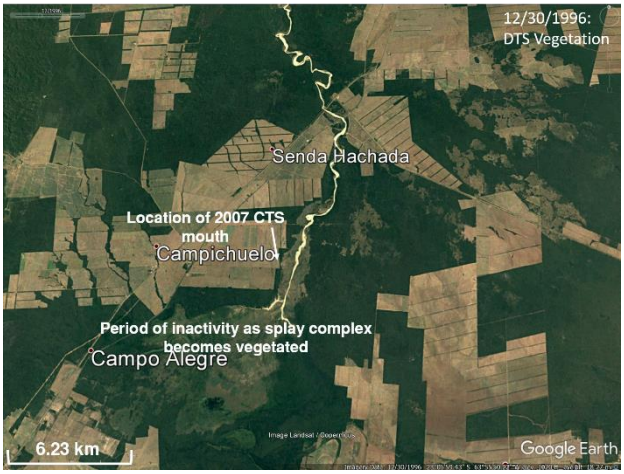

Figure A.13 Aerial photograph of the CTS complex, 12/30/1996 (Google Earth).

Figure A.14 Aerial photograph of the CTS complex, 12/30/1997 (Google Earth).

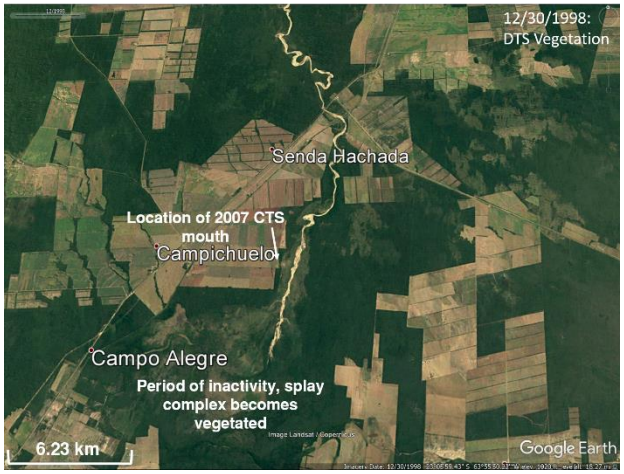

Figure A.15 Aerial photograph of the CTS complex, 12/30/1998 (Google Earth).

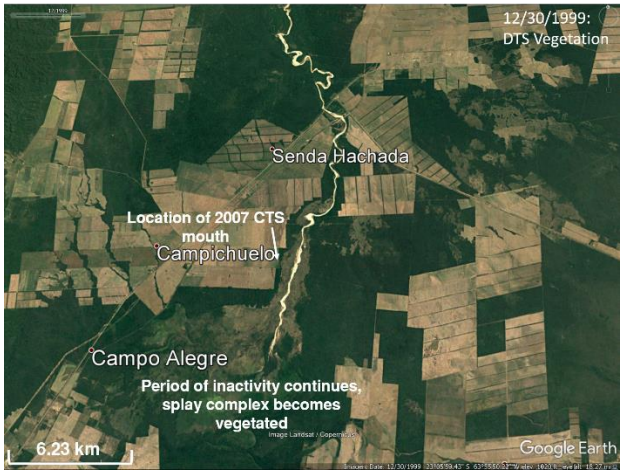

Figure A.16 Aerial photograph of the CTS complex, 12/30/1999 (Google Earth).

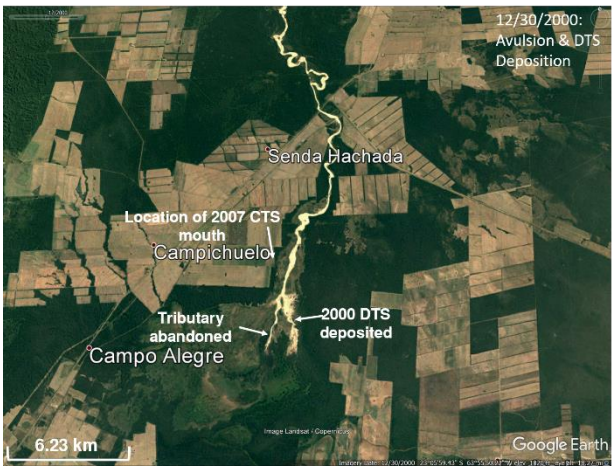

Figure A.17 Aerial photograph of the CTS complex, 12/30/2000 (Google Earth).

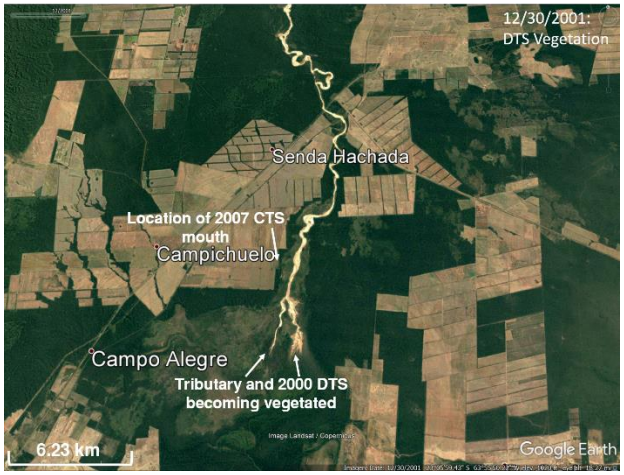

Figure A.18 Aerial photograph of the CTS complex, 12/30/2001 (Google Earth).

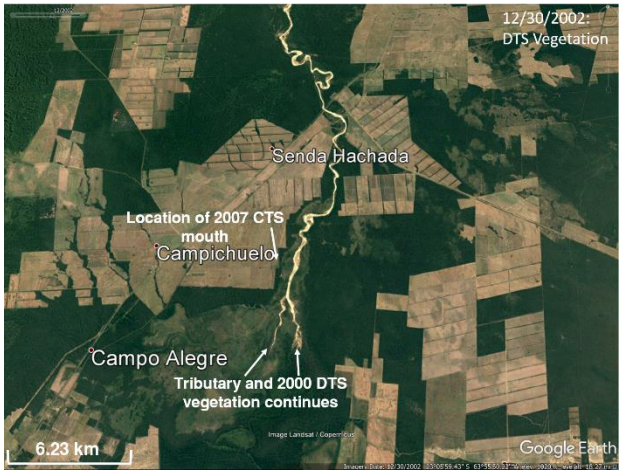

Figure A.19 Aerial photograph of the CTS complex, 12/30/2002 (Google Earth).

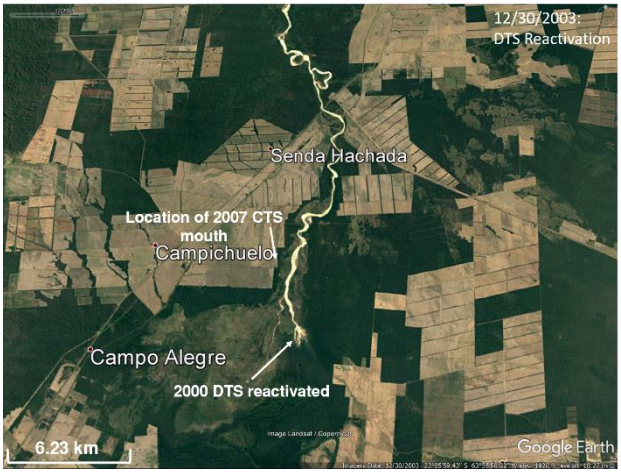

Figure A.20 Aerial photograph of the CTS complex, 12/30/2003 (Google Earth).

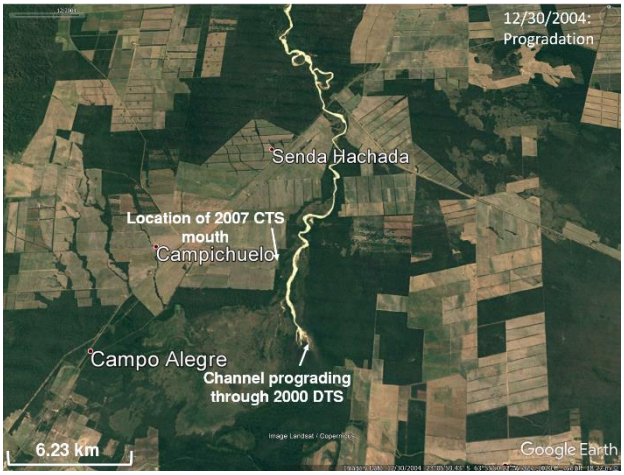

Figure A.21 Aerial photograph of the CTS complex, 12/30/2004 (Google Earth).

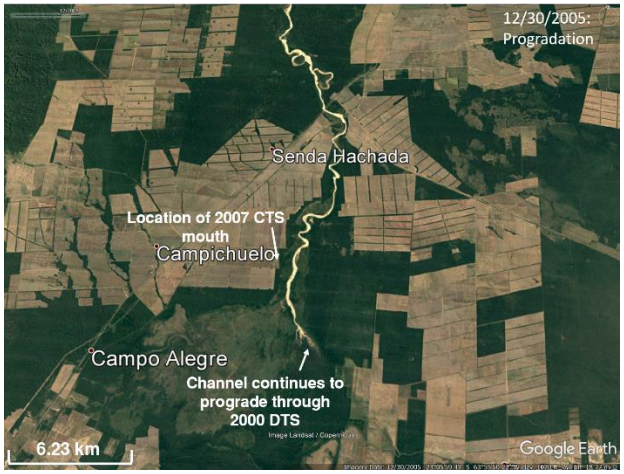

Figure A.22 Aerial photograph of the CTS complex, 12/30/2005 (Google Earth).

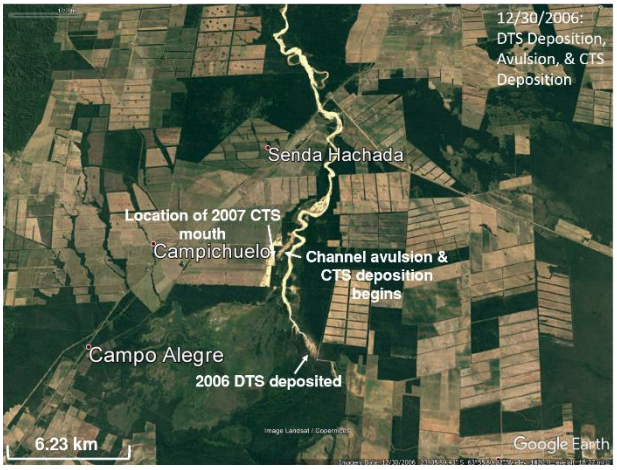

Figure A.23 Aerial photograph of the CTS complex, 12/30/2006 (Google Earth).

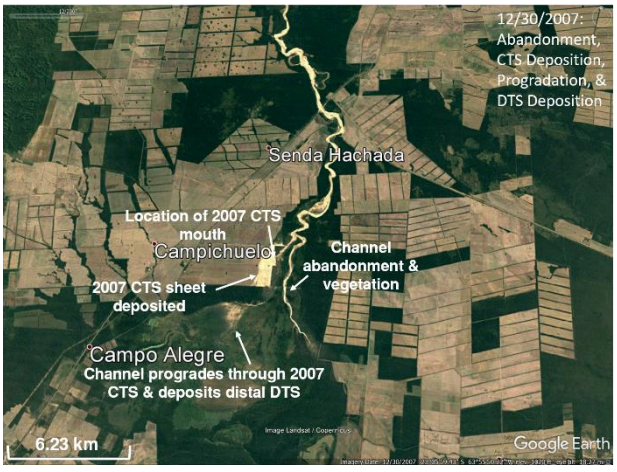

Figure A.24 Aerial photograph of the CTS complex, 12/30/2007 (Google Earth).

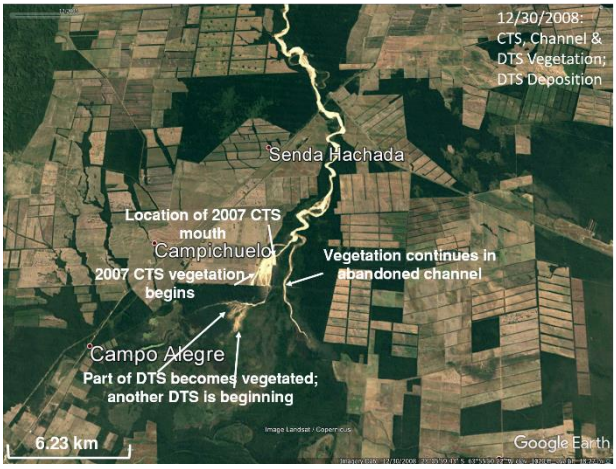

Figure A.25 Aerial photograph of the CTS complex, 12/30/2008 (Google Earth).

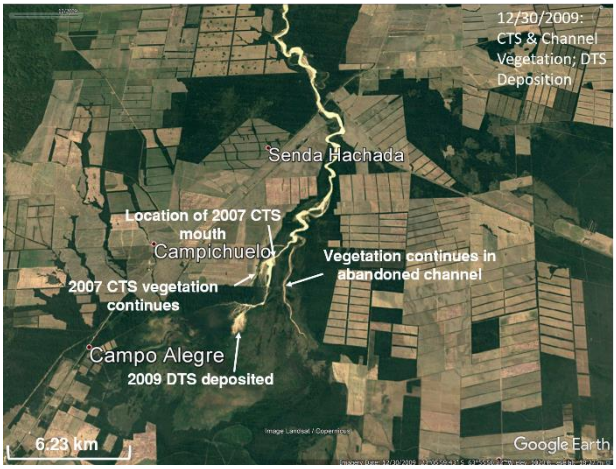

Figure A.26 Aerial photograph of the CTS complex, 12/30/2009 (Google Earth).

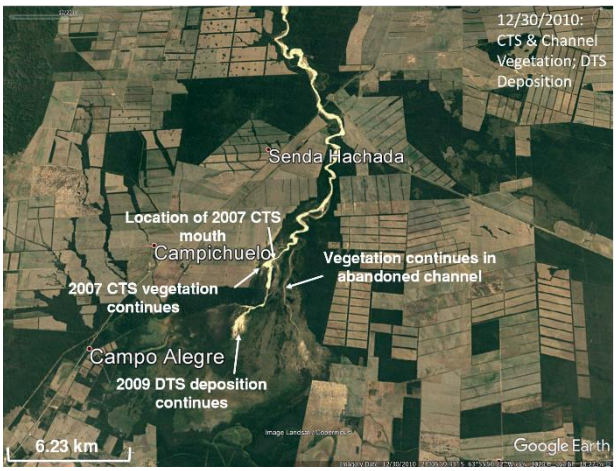

Figure A.27 Aerial photograph of the CTS complex, 12/30/2010 (Google Earth).

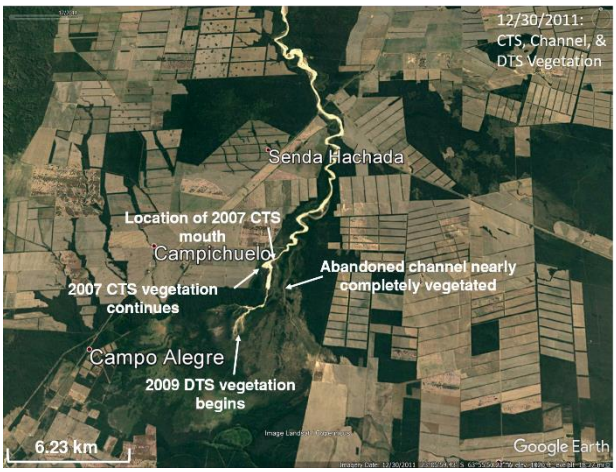

Figure A.28 Aerial photograph of the CTS complex, 12/30/2011 (Google Earth).

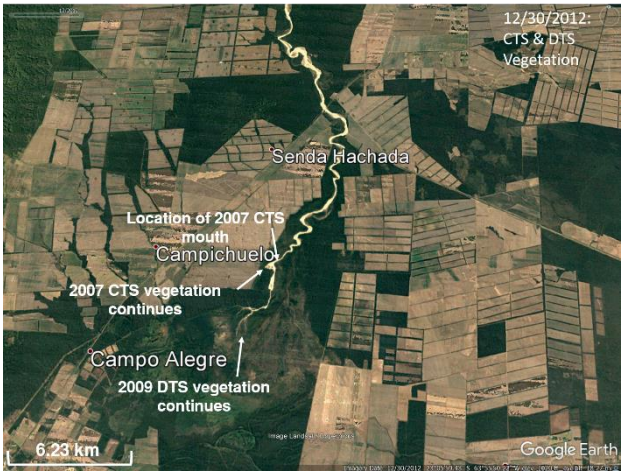

Figure A.29 Aerial photograph of the CTS complex, 12/30/2012 (Google Earth).

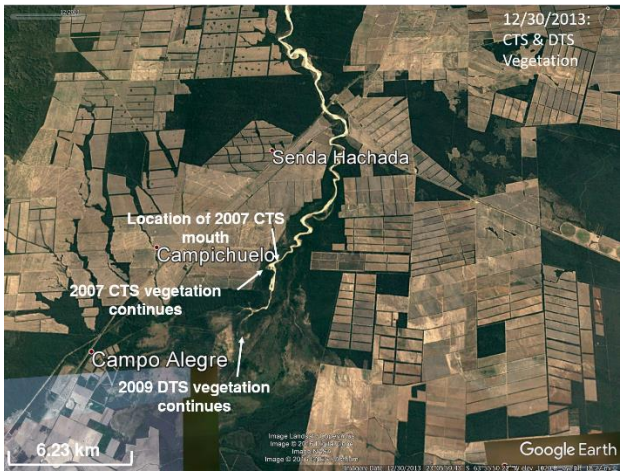

Figure A.30 Aerial photograph of the CTS complex, 12/30/2013 (Google Earth).

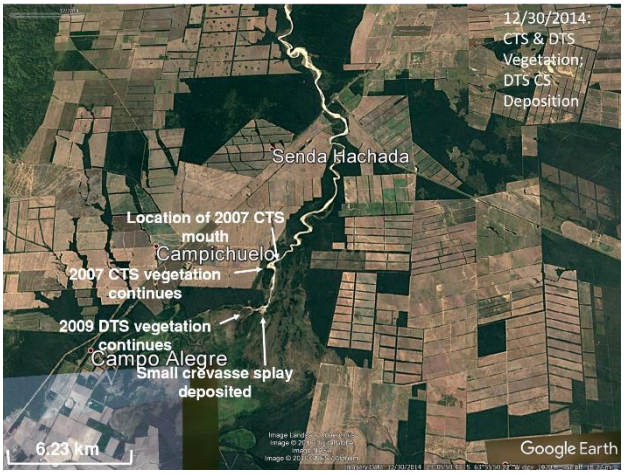

Figure A.31 Aerial photograph of the CTS complex, 12/30/2014 (Google Earth).

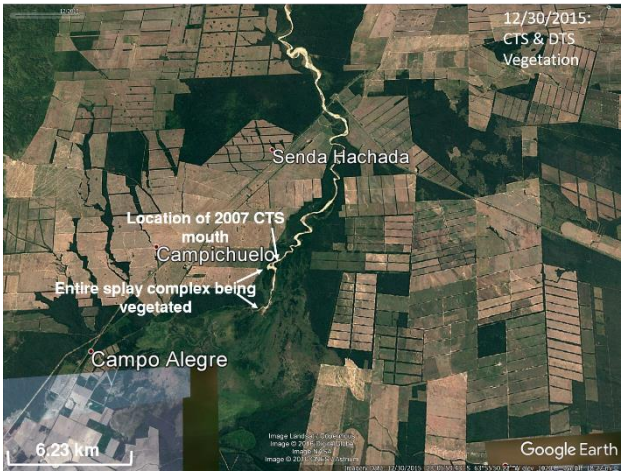

Figure A.32 Aerial photograph of the CTS complex, 12/30/2015 (Google Earth).

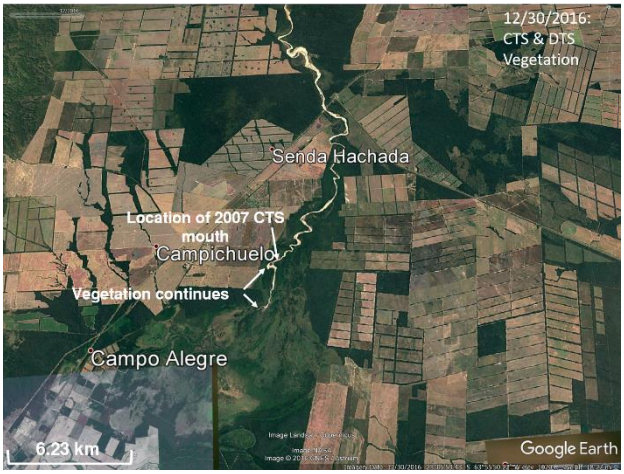

Figure A.33 Aerial photograph of the CTS complex, 12/30/2016 (Google Earth).

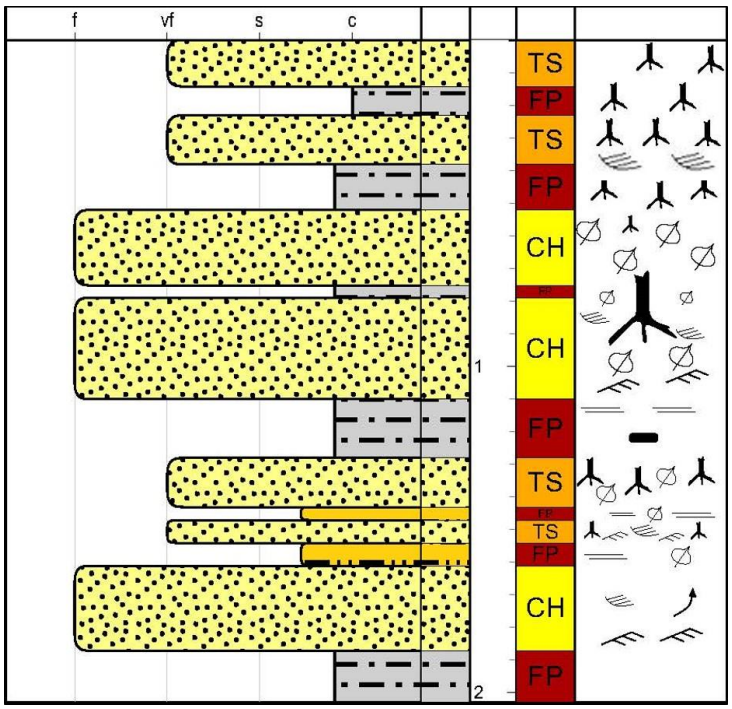

Figure A.34 Measured section of Lower Valdez outcrop. Section 1/7 moving east to west.

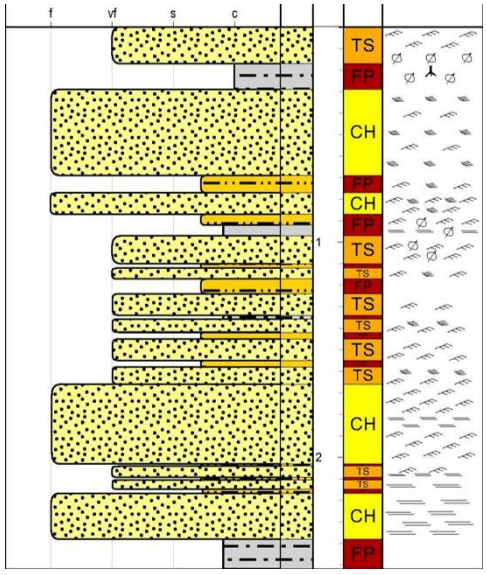

Figure A.35 Measured section of Lower Valdez outcrop. Section 2/7 moving east to west.

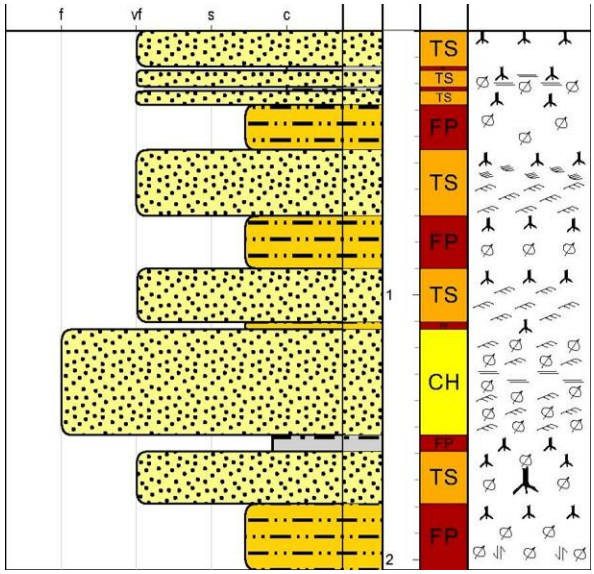

Figure A.36 Measured section of Lower Valdez outcrop. Section 3/7 moving east to west.

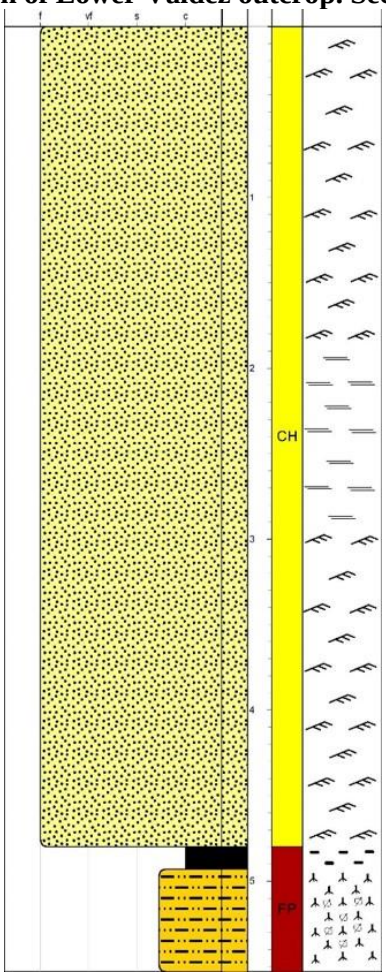

Figure A.36 Measured section of Lower Valdez outcrop. Section 4/7 moving east to west.

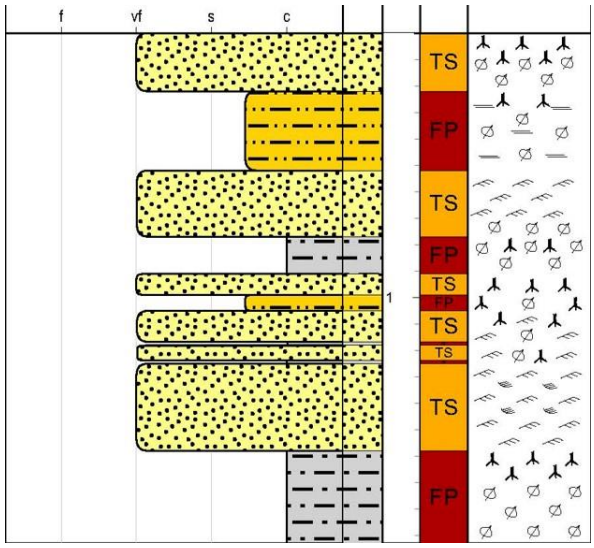

Figure A.37 Measured section of Lower Valdez outcrop. Section 5/7 moving east to west.

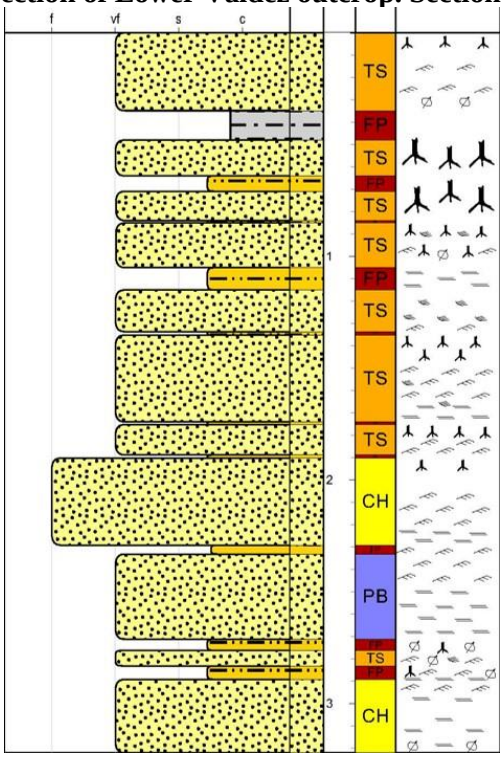

Figure A.38 Measured section of Lower Valdez outcrop. Section 6/7 moving east to west.

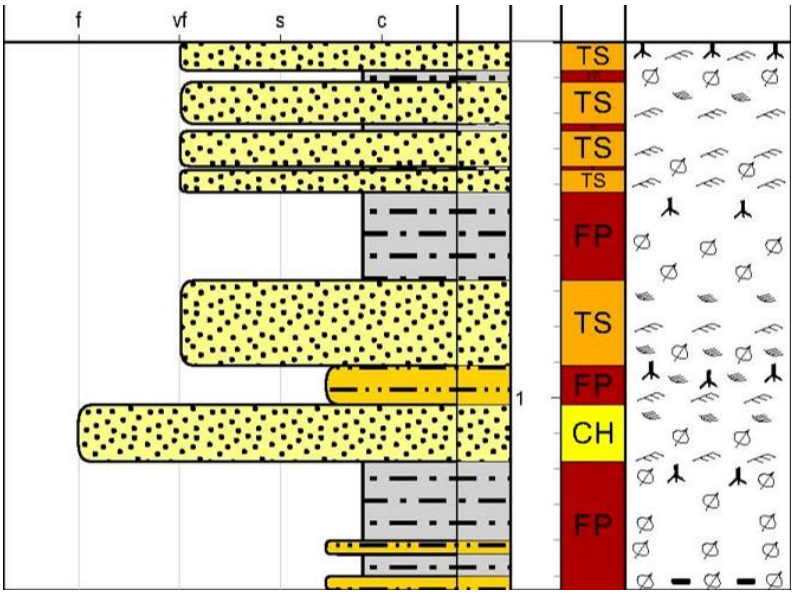

Figure A.39 Measured section of Lower Valdez outcrop. Section 7/7 moving east to west.

VITA

Graham Edward McGregor was born on October 15, 1992 in Wichita Falls, Texas to Bill and Katherine McGregor. He was born in raised in Wichita Falls and graduated from Rider High School in May of 2011.

Following high school graduation, Graham began his college career at The University of Texas in August of 2011. During the summer before his senior year, after completing UT Austin's field camp, he spent half of the summer as a geology intern at Wagner Oil Company in Fort Worth, Texas. He graduated from the Jackson School of Geosciences with a Bachelor of Science in Geology in May 2015.

Upon graduating, he found himself back in Fort Worth in August of 2015 where he began his Masters in Geology at Texas Christian University. During his time at TCU, he worked as a consultant at the TCU IT Helpdesk where he helped students, faculty and staff with any technological issues they may have had. At the beginning of his second semester, he began working part time as a geologist at Wagner Oil Company. Also served as a geology intern with Dale Operating Company during the summer of 2017.

ABSTRACT

HUMID TERMINAL SPLAYS AS SAND-SHEET RESERVOIRS: A FIRST LOOK AT THE MODERN, ANDEAN FORELAND, AND A NEW LOOK AT THE ANCIENT, RATON BASIN

By Graham E. McGregor
School of Geology, Energy and the Environment
Texas Christian University

John M. Holbrook, Professor of Geology

Richard Denne, Hunter Enis Chair of Petroleum Geology

Bo Henk, Adjunct Professor of Geology

Thin sand sheets presumed to be terminal splay bodies have potential to serve as hydrocarbon reservoirs. The few studies of terminal splays managed from arid systems has provided insight, but ground study of the humid equivalent is lacking. Deposited in the distal zone of a distributary fluvial system (DFS), the splay bodies are formed as rivers terminate from loss of slope into unconfined dispersive flow and deposit bed load as splays and advect mud to more distal floodplains. The splay sheets and floodplain together provide potential for both reservoir and seal. Terminal splay deposits were examined in a modern humid terminal splay system, Andean foreland of northern Argentina, and in ancient foreland deposits, Paleocene Raton Formation of the Colorado Raton Basin. The two locations are compared in terms of grain-size, sedimentary structures, geometry, and scale and see how they relate. I hypothesize that the two are going to have similar grain sizes, and that the sedimentary structures and geometries will also be analogous but expect them to be scaled down in the Raton Basin. The modern splay in Argentina is nearly 1.3 km wide and 1.9 km long and was deposited during a

single large flood in 2007. Cross sections generated by hand augers show an average thickness of 57.5 cm, and a consistently very fine-grained to lower medium-grained sand texture throughout. Total sand deposited in the flood event is ~ 1.4 million cubic meters over ~2.37 million square meters, and accumulates over earlier splay deposits separated by weakly developed soils that are locally removed by splay incision. Subsequent dissection of the splay permits examination of sedimentary structures, which are dominantly climbing ripples, planar laminations, and cross sets, but climbing antidunes are locally found near the splay apex. Ancient terminal splays of the Raton Formation are made of thinner sand sheets and tend to have thicker muddy floodplain deposits between. Grain-size distribution, sheet geometry, and sedimentary structures however are consistent between the modern and ancient examples. Both the Argentina and Raton examples reflect the distal end of a humid Distributive Fluvial System, however, the Raton system appears to have been of smaller scale. This is consistent with the comparatively smaller scale of the Raton vs. Andean tectonic system.